

# Impact of individual early life traits in larval dispersal: a multispecies approach using backtracking models.

1 **Héctor Torrado**<sup>1,2 \*</sup>, **Baptiste Mourre**<sup>3</sup>, **Núria Raventos**<sup>1</sup>, **Carlos Carreras**<sup>2</sup>, **Joaquín Tintoré**<sup>3,4</sup>,  
2 **Marta Pascual**<sup>2+</sup>, **Enrique Macpherson**<sup>1+</sup>

3

4 <sup>1</sup>Centre d'Estudis Avançats de Blanes (CEAB-CSIC), Blanes, Girona, Spain.

5 <sup>2</sup>Department de Genètica, Microbiologia i Estadística and IRBio, Universitat de Barcelona,  
6 Barcelona, Spain.

7 <sup>3</sup>SOCIB, Balearic Islands Coastal Observing and Forecasting System. Palma, Illes Balears, Spain.

8 <sup>4</sup>Institut Mediterrani d'Estudis Avançats (IMEDEA-UIB-CSIC), Esporles, Illes Balears, Spain.

9 <sup>+</sup>Both authors contributed equally as senior researchers and should be considered to be at the same  
10 position

11 \* **Correspondence:**

12 Héctor Torrado

13 h.torrado@hotmail.com

14 **Keywords:** Fish larvae, Oceanographic models, Lagrangian particle dispersion, Individual-based  
15 model, Early life traits, Otolith reading.

16 **Abstract**

17 Dispersal is a key process shaping species population structure. In demersal marine fishes, which  
18 usually have sedentary adult phases, dispersion relies on drifting larval stages. However, the dynamics  
19 and seasonal variability of seawater masses can greatly determine the connectivity patterns of these  
20 species along the same geographic gradient. For this reason, detailed information on the release  
21 moment of larvae is needed to obtain accurate patterns of connectivity. In this study, we performed  
22 backtracking Lagrangian particle dispersion simulations, with individual-based early life traits data,  
23 obtained from otolith reading for 1,413 juveniles of nine fish species belonging to three families  
24 (Sparidae, Pomacentridae and Labridae). For each species, individuals had been sampled from four to  
25 seven localities in the western Mediterranean Sea between the Gulf of Lion to the Gibraltar Strait.  
26 These nine species reproduce in different seasons of the year and their pelagic larval duration (PLD)  
27 range from 7 to 43 days. We identified three hydrodynamic units separated by oceanographic  
28 discontinuities (Balearic Sea, West Algerian Basin and Alboran Sea) with low settler's exchange  
29 according to our simulations, independently of the PLD and reproductive season of the species.  
30 Hatching date and PLD showed significant effects on larval dispersal distance and orientation, both at  
31 the intraspecific and interspecific levels, highlighting the importance of these variables in determining  
32 the geographic origin of individuals. Our multispecies modelling approach adds a step forward for an  
33 accurate description of larval dispersion and recruitment, key to understand population resilience and  
34 define management strategies.

## 35 **1 Introduction**

36 In benthic and pelagic marine habitats hydrodynamic processes, e.g. temperature, productivity  
37 gradients and turbulent oceanographic features, interact with biological processes affecting species  
38 distribution and communities (Cowen, 2002). Physical processes are usually highly variable and their  
39 role in generating and maintaining patterns in community structure are essential in marine ecology  
40 studies (Shanks and Brink, 2005; White et al., 2019). There is a close relationship between temporal  
41 and spatial scales of this physical variability and the apparent high levels of asymmetry and  
42 stochasticity in biological processes (Ayata et al., 2010).

43 Most marine organisms, including most benthic fishes, have low-dispersive adult phases and  
44 high-dispersive pelagic larval stages. This dual life history makes early life processes especially pivotal  
45 to marine ecology, influencing not only dispersal but also settlement rates, with the resulting effects  
46 on community structure (Leis, 1991). In the plankton, the duration of the larval pelagic stage (PLD)  
47 determines the length of time that larvae are subject to movement by currents, winds or eddies, and  
48 other physical processes, influencing dispersal distances (Gaines et al., 2007; Kinlan et al., 2005;  
49 Shanks, 2009). PLD is a key biological factor for larval dispersion since longer PLDs potentially allow  
50 larvae to travel larger distances (Selkoe and Toonen, 2011; Shanks, 2009; Trembl et al., 2012). PLD can  
51 also be influenced by the spawning periodicity or seasonality, potentially affecting dispersal and  
52 connectivity (Kough and Paris, 2015), suggesting that hatching time can also be important in dispersal  
53 patterns. The dispersive planktonic larval phase(s) is considered as a “black box” in part due to our  
54 limited understanding of the relationships between larvae and their environment (Cowen and  
55 Sponaugle, 2009; Paris and Cowen, 2004).

56 Numerous physical mechanisms, e.g. currents, eddies, waves, have been associated with the  
57 transport of larvae (Banks et al., 2007; Selkoe et al., 2010), emphasising the importance of their  
58 temporal and spatial variability on the larval transport and settlement dynamics (S. Sponaugle and

59 Cowen, 1996). On the other hand, the release of larvae in the plankton, e.g. hatching period, and their  
60 settlement time, show also a large temporal and spatial variability. The coupling of these physical and  
61 biological processes are difficult to identify, adding an element of stochasticity to these events  
62 (Sponaugle et al., 2005). Therefore, the difficulty to identify these fundamental physical-biological  
63 interactions, and how they change along space and time, remains scarcely studied, limiting a more  
64 complete knowledge of dispersal processes.

65 The displacements produced in the course of this pelagic period have been frequently modelled  
66 to describe the potential dispersal capabilities of species using Lagrangian-based larval dispersal  
67 modelling (Andrello et al., 2017; Calò et al., 2018; Rossi et al., 2014; Schunter et al., 2011a; Trembl et  
68 al., 2012). Classic approaches use forward simulations, releasing particles from potential source areas  
69 and following the current fields to their settlement areas. This methodology has been used to study  
70 propagule dispersal and potential impact of climate change (Andrello et al., 2015) or spatial and  
71 temporal variability of larval dispersion (Barbut et al., 2019; Di Franco et al., 2012; Ospina-Alvarez et  
72 al., 2015). Nevertheless, when the study focuses on particular sampling areas, an alternative approach  
73 consists in backtracking the particles from the settlement areas by running the oceanographic model  
74 back in time in order to find their potential origin or source areas. Backtracking approximations have  
75 been used in larval dispersal modelling at population level to evaluate the effect of oceanographic  
76 structures in the area (Holliday et al., 2012), for potential hatch area identification (Calò et al., 2018;  
77 Christensen et al., 2007; Fraker et al., 2015), recruitment predictions for fisheries management (Allain  
78 et al., 2007) and to reconstruct the environmental history associated to larval growth rate (Payne et al.,  
79 2013; Ross et al., 2012).

80 Recently, these models have included some aspects related to larval behaviour. The natatory  
81 capacities are reduced at the initial pelagic phases, and consequently their transport is mainly passive  
82 and driven by the ocean currents in the area (Leis, 2007). However, larvae experience an ontogenetic

83 improvement of swimming capabilities and can modify their trajectories at later pelagic phases through  
84 vertical migrations (Leis, 2007; Paris and Cowen, 2004) and horizontal orientated swimming  
85 (Faillettaz et al., 2018; Staaterman et al., 2012). The mechanisms allowing larval orientation in open  
86 waters are badly known, although they could have a notable impact on their final destination, and some  
87 authors have suggested the use of odour, sun, or magnetic fields (Bottesch et al., 2016; Faillettaz et al.,  
88 2015; Leis et al., 2014; Mouritsen et al., 2013; O'Connor and Muheim, 2017; Paris et al., 2013).

89 In fish larval dispersal studies, the high temporal and spatial variability of the oceanographic  
90 currents makes the accurate estimation of the dates and duration of the larval periods especially  
91 important. Otolith (ear bone) microstructure analysis provides a useful tool to obtain this information  
92 at individual level. Otoliths of most temperate fishes show daily growth rings and lay a clear settlement  
93 band when the individuals change from the pelagic to the benthic stage (Raventos and Macpherson,  
94 2005, 2001; Wilson and McCormick, 1999). Using otolith reading, we can obtain the early life history  
95 of each settler, including the day of hatching and settlement, and the PLD. Therefore, the combination  
96 of otolith-inferred accurate early-life traits and high-resolution models of oceanographic currents  
97 represents an interesting strategy to analyse the dispersal patterns of individual fish larvae.

98 The Western Mediterranean Sea provides a good system to evaluate the effect of oceanographic  
99 processes on larval dispersal (Figure 1). It is connected with the Atlantic Ocean through the Strait of  
100 Gibraltar, where there is an inflow of surface Atlantic water and outflow of deeper Mediterranean water  
101 (Millot, 1999; Millot and Taupier-Letage, 2005). The circulation pattern and topography along the  
102 southern and eastern coasts of the Iberian Peninsula originate three main oceanographic discontinuities  
103 in the study area (Figure 1): the Almeria-Oran Front (AOF), the Ibiza Channel (IC) and the Balearic  
104 Front (BF). The AOF is a large scale density front located 400 km east of the Gibraltar Strait (GS) and  
105 formed by the convergence of the main jet of incoming Atlantic water and waters having recirculated  
106 in the Mediterranean Sea (Tintoré et al., 1988). The strength of the AOF varies with the changes

107 affecting the Eastern Alboran Gyre (Renault et al., 2012). East of the AOF, the main current carries  
108 Atlantic water eastward along the African coast. Part of this water continues towards the eastern basin  
109 through the Sicily Channel, while the other part flows through the Tyrrhenian Sea (Astraldi et al., 1999;  
110 Millot and Taupier-Letage, 2005). The circulation in the Western basin is mainly cyclonic, with the  
111 Northern Current flowing south-westward along the French and Spanish coasts and bifurcating when  
112 reaching the south of the Balearic Sea (Garcia Lafuente et al., 1995; Salat, 1996). The IC, 80 km wide  
113 and 800 m depth, corresponding to the passage intersecting the Balearic topographic ridge between  
114 Ibiza and the Iberian Peninsula at Cape La Nao, is a key choke point with important exchanges between  
115 waters of recent Atlantic origin in the south and saltier waters of Mediterranean characteristics in the  
116 northern side (Heslop et al., 2012; Pinot et al., 2002). Finally, the part of the flow directed north-  
117 eastward along the northern Balearic shelf edge forms a well-defined density front, the BF, present in  
118 the upper 200 m (Figure 1). The dynamic behaviour of these oceanographic discontinuities generate  
119 significant intra- and inter-annual variability (Tintoré et al., 2019) that can affect larval dispersal  
120 patterns (Su Sponaugle and Cowen, 1996).

121 In the present work, and using a multispecies approach, we evaluated how differing hatching  
122 dates and pelagic larval durations interact with variable oceanographic features to influence larval  
123 dispersal patterns throughout the Western Mediterranean. We modelled individual-based potential  
124 larval movement of 1,413 settlers of nine common coastal fish species along the western Mediterranean  
125 Sea, reproducing in different seasons and with different PLD. We used individual-based information  
126 on early life traits (day of hatching and settlement, and PLD) from otoliths readings (Raventos et al.,  
127 2021). We backtracked each settler running Lagrangian trajectories back in time using currents from a  
128 high-resolution model of the Western Mediterranean Sea (Juza et al., 2016; Mourre et al., 2018), in  
129 order to find their potential origin and to evaluate the effect of the oceanographic variability. Our  
130 specific objectives were: a) to determine the effect of the currents and oceanographic structures and

131 their seasonal variability on dispersal patterns and b) to assess the influence of interspecific and  
132 intraspecific variation of hatching date and PLD on dispersal potential of the nine species. We  
133 hypothesized that the dispersal patterns of fishes would be influenced by variations in hatching date  
134 and PLD, between species as well as within species, coupled with changes in oceanographic conditions,  
135 and thus should be considered for accurately modelling dispersal.

136

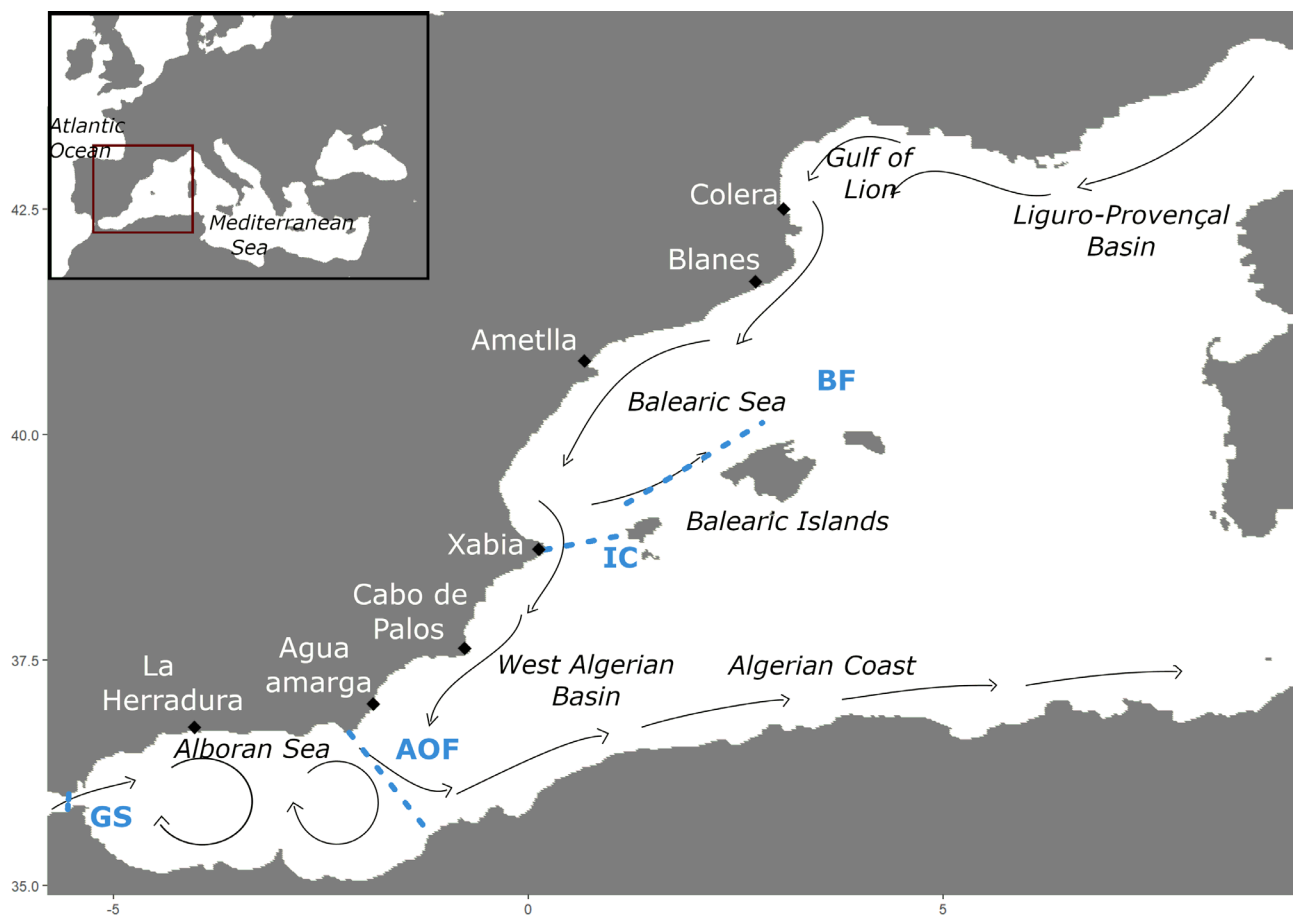
## 137 **2 Materials and Methods**

### 138 **2.1 Species data**

139 In the present work we modelled the dispersal capacity of nine coastal co-occurring fish species from  
140 three different families along the western Mediterranean Sea: (1) Sparidae, the common two-banded  
141 seabream *Diplodus vulgaris*, the white seabream *D. sargus*, the sharpsnout seabream *D. puntazzo*, the  
142 salema *Sarpa salpa* and the saddled seabream *Oblada melanura*; (2) Pomacentridae, the damselfish  
143 *Chromis chromis*; (3) Labridae, the Mediterranean rainbow wrasse *Coris julis*, the ocellated wrasse  
144 *Symphodus ocellatus*, and the East Atlantic peacock wrasse *S. tinca*.

145 We based our study on the individualized early life traits information of 1,413 settlers from these nine  
146 species (Table S1) obtained in the study of (Raventos et al., 2021): *Diplodus vulgaris* (n=174), *D.*  
147 *sargus* (n=175), *D. puntazzo* (n=206), *Sarpa salpa* (n=72), *Oblada melanura* (n=216), *Chromis*  
148 *chromis* (n=146), *Coris julis* (n=150), *Symphodus ocellatus* (n=177) and *S. tinca* (n=97). Settlers of all  
149 sizes were collected at the end of the settlement period of each species to ensure the representation of  
150 the entire hatching period. We mostly restricted our analyses to individuals born during the same  
151 reproductive period for a given species with the exception of *S. tinca* where the samples from Blanes  
152 were included despite being from a different year, to be able to model at least four locations for each  
153 species, and *S. ocellatus* where the samples from La Herradura were used (Table S1). For each  
154 individual, the age at sampling was determined by counting the total number of bands in their otoliths,

155 from core to margin. Their individual PLD and settlement day was determined by counting the number  
156 of daily rings visible between the core and the settlement mark, and ages were used to calculate their  
157 day of birth. The settlers of these nine species were sampled at seven locations of the Western  
158 Mediterranean Sea, from Colera in the Gulf of Lion (42°40'N, 3°11'E) to La Herradura (36°44'N,  
159 3°44'W) in the Alboran Sea (Figure 1, Table S1). Some species were not collected in all locations (e.g.  
160 *Sarpa salpa*, 4 locations) due to the lack of settlers' availability during the sampling periods in those  
161 localities. The nine selected species have different pelagic larval duration (PLD) and reproduce in  
162 different seasons of the year, with no large differences found between localities within species (Figure  
163 2, Table S1).



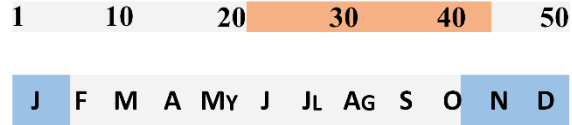
164

165 Figure 1. Map of the sampling locations and main schematic oceanographic currents in the Western  
166 Mediterranean Sea. The red square in the map of Europe correspond to the enlarged map of the  
167 analysed area. Diamonds: sampling localities; Dashed blue lines indicate oceanographic barriers; BF:

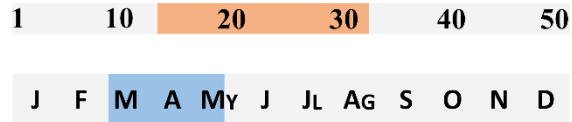
168 Balearic front; IC: Ibiza channel; AOF: Almeria-Oran front; GS: Gibraltar Strait. Currents are  
 169 represented as thin black lines with arrows identifying its main direction (Millot, 1999).

170

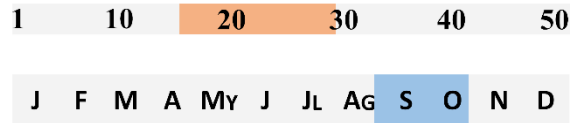
***Diplodus vulgaris***



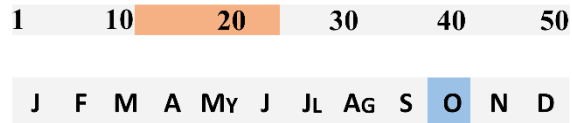
***Diplodus sargus***



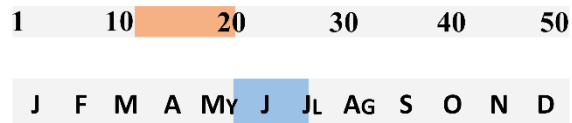
***Diplodus puntazzo***



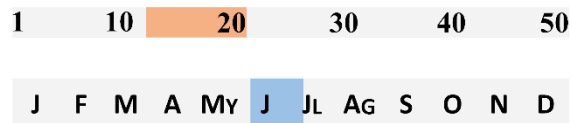
***Sarpa salpa***



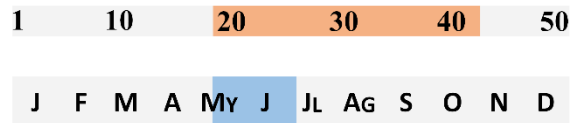
***Oblada melanura***



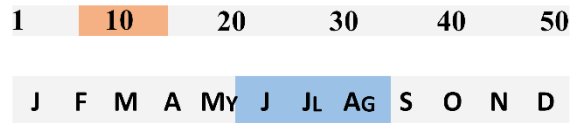
***Chromis chromis***



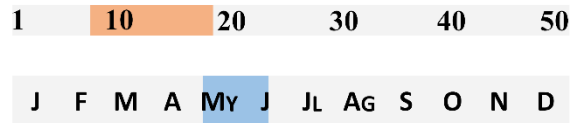
***Coris julis***



***Symphodus ocellatus***



***Symphodus tinca***



171



172 Figure 2. Ranges of Pelagic larval duration (PLD) in days (orange bar) and Hatching season in months  
173 (blue bar) for each species obtained from (Raventos et al., 2021). Species' images obtained from  
174 (Bauchot, 1987; Schneider, 1990).

## 175 2.2 Modelling

176 For our modelling analyses we used the ocean current fields provided by the Western Mediterranean  
177 OPERational forecasting system (WMOP) (Juza et al., 2016; Mourre et al., 2018), developed at the  
178 Balearic Islands Coastal Observing and Forecasting System ([www.socib.es](http://www.socib.es), Tintoré et al., 2013).  
179 WMOP uses 5km-resolution surface atmospheric forcing from the HIRLAM model of the Spanish  
180 Meteorological Agency AEMET, with a temporal resolution of 3h before March 2017 and 1h  
181 afterwards. In particular, WMOP near-surface currents include the effects of the winds blowing on the  
182 sea surface. The boundary conditions are provided by the outputs of the larger scale Mediterranean  
183 model from the Copernicus Marine Service (Clementi et al., 2017). WMOP has a spatial coverage from  
184 Gibraltar strait to Sardinia Channel (35°N-44.5°N, 6°W-9°E) and a horizontal resolution of around  
185 2 km and 32 sigma-levels in the vertical dimension. Detailed assessments of the WMOP model from  
186 the basin to the coastal scales have demonstrated that the model was able to represent the mean large-  
187 scale surface circulation and the associated modes of variability with a satisfactory level of realism  
188 (Aguiar et al., 2020; Juza et al., 2016; Mourre et al., 2018). Comparisons with satellite altimetry have  
189 shown that the model was generating realistic statistics of large eddies and accurate magnitude and  
190 spatial variability of eddy kinetic energy. At the coastal scales and based on surface drifter data, the  
191 model was found to represent small scale processes such as topographically driven coastal eddies or  
192 localized sea breeze effects close to Mallorca Island. High-Frequency (HF) radar data have  
193 demonstrated that the model was able to properly represent the position of the Northern Current and  
194 the coastal flow intensification in the coastal region off Ebro delta. In the Ibiza Channel, while some  
195 overestimation of the northward surface flow was highlighted based on HF radar measurements, the

196 seasonal and interannual variability of the Western Intermediate Water was positively evaluated in the  
197 model using underwater glider time series (Juza et al., 2019). Daily updated comparisons with satellite  
198 SST, altimetry, ARGO profiles, mooring time series, glider sections and coastal currents from HF  
199 radars in 3 different locations (Gibraltar strait, Ibiza Channel and Ebro Delta) are available at  
200 <https://socib.es/?seccion=modelling&facility=wmedvalidation>.

201 Backtracking individual-based Lagrangian particle dispersion simulations were performed with the  
202 WMOP data using the TRACMASS software (Döös and Jönsson, 2013), implemented through the  
203 TracPy interface (Thyng and Hetland, 2014). Each individual simulation considered the following data:  
204 release point (sampling locality), date (settlement date) and simulation duration (pelagic larval  
205 duration) based on each individual sample and otolith data. Simulations were then performed for  
206 different periods of the year in 2014, 2015 and 2017 according to individual data (Table S1, for full  
207 otolith data access, see Raventós et al., 2021). For each individual we simulated the release and  
208 movement of  $10^3$  particles from their settlement site to their potential source origin during their  
209 settlement and hatch dates. We added random velocity fluctuations to simulations in order to account  
210 for model uncertainties and unresolved processes. The magnitude of the random turbulent velocities  
211 was the result of the specific calibration experiments performed in the framework of the development  
212 of the TRACMASS algorithm (Döös et al., 2011; Döös and Engqvist, 2007), combined with our own  
213 experience with trajectory modelling using currents from the 2km resolution WMOP model when  
214 compared to real drifters (Mourre et al., 2018). The random coefficients were fixed so as to produce a  
215 standard deviation of random velocity fluctuations which reaches 0.8 times the standard deviation of  
216 the WMOP model velocities along the trajectories. During the last half of the larval period (first part  
217 of the backtracking simulation), we added a velocity vector towards the coastline, based on the larval  
218 Critical speed ( $U_{crit}$ ) of each species, representing larval swimming abilities.  $U_{crit}$  values were  
219 obtained from laboratory studies, including the same or closely related species for each family,

220 Sparidae and Pomacentridae (Faillettaz et al., 2018), and Labridae (Leis et al., 2011). We considered  $\frac{1}{2}$   
221  $U_{crit}$  as the mean velocity directed towards the coast when the particle was less than 5 km off the  
222 coastline. Therefore, we considered that within this distance larvae are capable of a good directional  
223 orientation due to the detection of more precise clues like odour or sound (Kingsford et al., 2002). For  
224 grid points more than 5km off the coastline, we assumed a velocity of  $\frac{1}{4} U_{crit}$ . Reducing velocities at  
225 further distances are the result of assuming a minor net displacement towards the coast due to reduced  
226 orientation capabilities and considering a bigger importance of individual stochasticity. Larvae of most  
227 of the studied species are usually concentrated in the upper 10 m of the water column, with very limited  
228 or negligible diel vertical migration (Sabatés and Olivar, 1996). Thus, particles representing fish larvae  
229 were simulated at fixed depths for the full advection period (Table S1) following observed mean larval  
230 depth (Olivar et al., 2010; Sabatés and Olivar, 1996).

231 In order to get insights into the impact of the oceanographic variability and evaluate the extent  
232 to which the year of study represents a typical current field, we have analysed the transport across the  
233 two oceanographic discontinuities (IC and AOF) separating the three hydrodynamic units present in  
234 the area (see results) from 2014 to 2018. The transports were computed at AOF (from -2.13E/36.75N  
235 to -0.79E/35.77N) and IC (from -0.15E/39N to 1.31E/39N) from model surface to bottom, separating  
236 northward and southward flows and integrating the product of model cross-section velocities by the  
237 surface of 2km-long cells.

238

### 239 2.3 Data analyses

240 We generated a total of 1000 backtracking particle trajectories for each of the 1,413 sampled  
241 individuals of the nine species. Since the studied species do not live nor reproduce in open sea, we only

242 kept for posterior analyses those particles originating in coastal waters (less than 2 km to the nearest  
243 land point) in the backtracking simulations, using nn2 function in the R package ‘RANN’ 2.6.1 (Arya  
244 et al., 2019). We plotted potential origin maps of settlers for each species in R 3.4.4 (R Core Team,  
245 2018) using the following packages: ‘ncdf4’ 1.16 (Pierce, 2017) for netCDF files reading and  
246 processing, ‘reshape’ 0.8.7 (Wickham, 2007) and ‘dplyr’ 0.7.8 (Wickham et al., 2018) for data  
247 reorganization, ‘magrittr’ 1.5 (Bache and Wickham, 2014) for function construction, ‘rgdal’ 1.3-1  
248 (Bivand et al., 2018) for geoprocessing and ‘ggplot2’ 3.1.0 (Wickham, 2016) for plotting. Furthermore,  
249 we plotted the mean current velocity of the WMOP for each species across its planktonic period  
250 assessed from the otolith data with the same methodology, using a ‘viridis’ R package scale (Garnier,  
251 2018) for colour scale construction.

252 For each individual, we calculated the mean dispersal distance and orientation considering the  
253 backtracking simulations originating in coastal waters. The angle of each particle was defined in  
254 relation to the Northwest in each sampling locality to avoid that the range of potential orientations  
255 within any location included the zero value, and thus this parameter always increases as the direction  
256 changes clockwise. In order to evaluate the effect of PLD and hatching date on mean dispersal distances  
257 and orientations we performed generalized lineal mixed model (GLMM) tests with the R package  
258 ‘lme4’ 1.1-23 (Bates et al., 2015). We first built an analysis with all data considering species and  
259 locality as random factors (Dispersal distance/Dispersal orientation ~ PLD + Hatching date + Species  
260 + Locality). Additionally, we carried out an analysis for each species separately to assess the mean  
261 dispersal distance and orientation as a function of PLD and hatching date while defining localities as a  
262 random factor (Dispersal distance/Dispersal orientation ~ PLD + Hatching date + Locality).

263 To assess the effect of oceanographic discontinuities on dispersal patterns we considered three sampled  
264 areas and seven source zones for simulated particles. We defined the three sampled areas as the three  
265 oceanographic regions separated by the oceanographic discontinuities along the study area (Figure 1):

266 (1) Alboran Sea: from the Gibraltar Strait (GS) to the Almeria-Oran Front (AOF), (2) West Algerian  
267 Basin: Iberian Peninsula area from the AOF to the Ibiza Channel (IC), and (3) Balearic Sea: Iberian  
268 Peninsula area from IC to Gulf of Lion. On the other hand, we delimited the seven potential source  
269 coastal areas (Figure 1): (1) Atlantic Ocean (Atlantic particles arriving through GS), (2) Alboran Sea  
270 (from GS to AOF), (3) West Algerian Basin (Iberian peninsula from AOF to IC), (4) Algerian coast  
271 (northern Africa from AOF towards the east), (5) Balearic Sea (Iberian peninsula from IC to Gulf of  
272 Lion), (6) Balearic Islands and (7) Liguro-Provençal Basin (from the Gulf of Lion towards the  
273 northeast). For each species we tested for differences in individual mean dispersal distances between  
274 areas using a Kruskal-Wallis test and a Dunn post-hoc test in R. We evaluated with the same test the  
275 variability of oceanographic transport across the IC and AOF in different years (2014-2017) during the  
276 whole pelagic period for each species (considering Hatching date and PLD according to our data). We  
277 plotted in a chord diagram the links between the source and sample areas with the R package ‘circlize’  
278 0.4.9 (Gu et al., 2014).

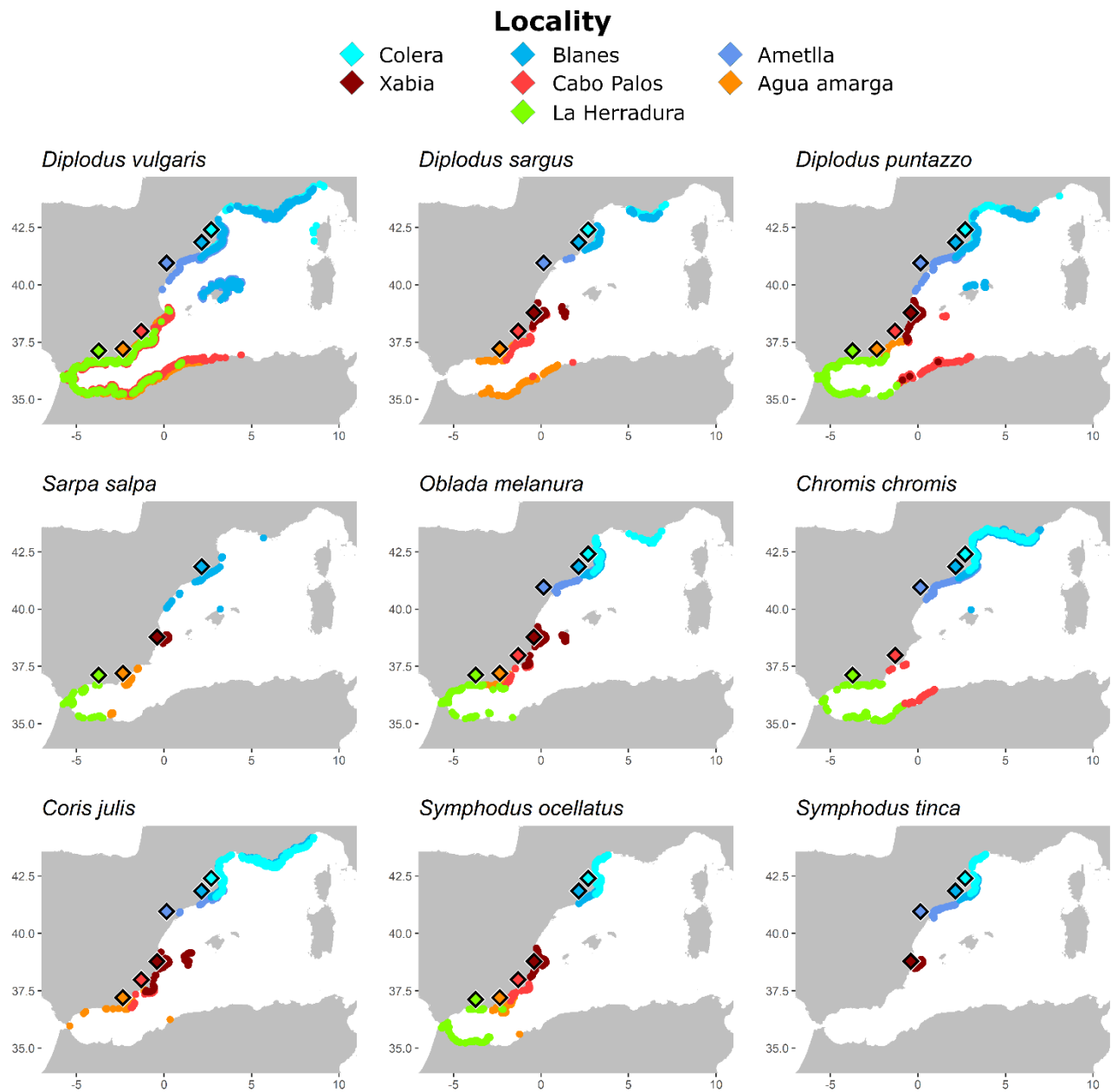
279

## 280 **3 Results**

### 281 **3.1 Hydrographic setting and backtracking trajectories**

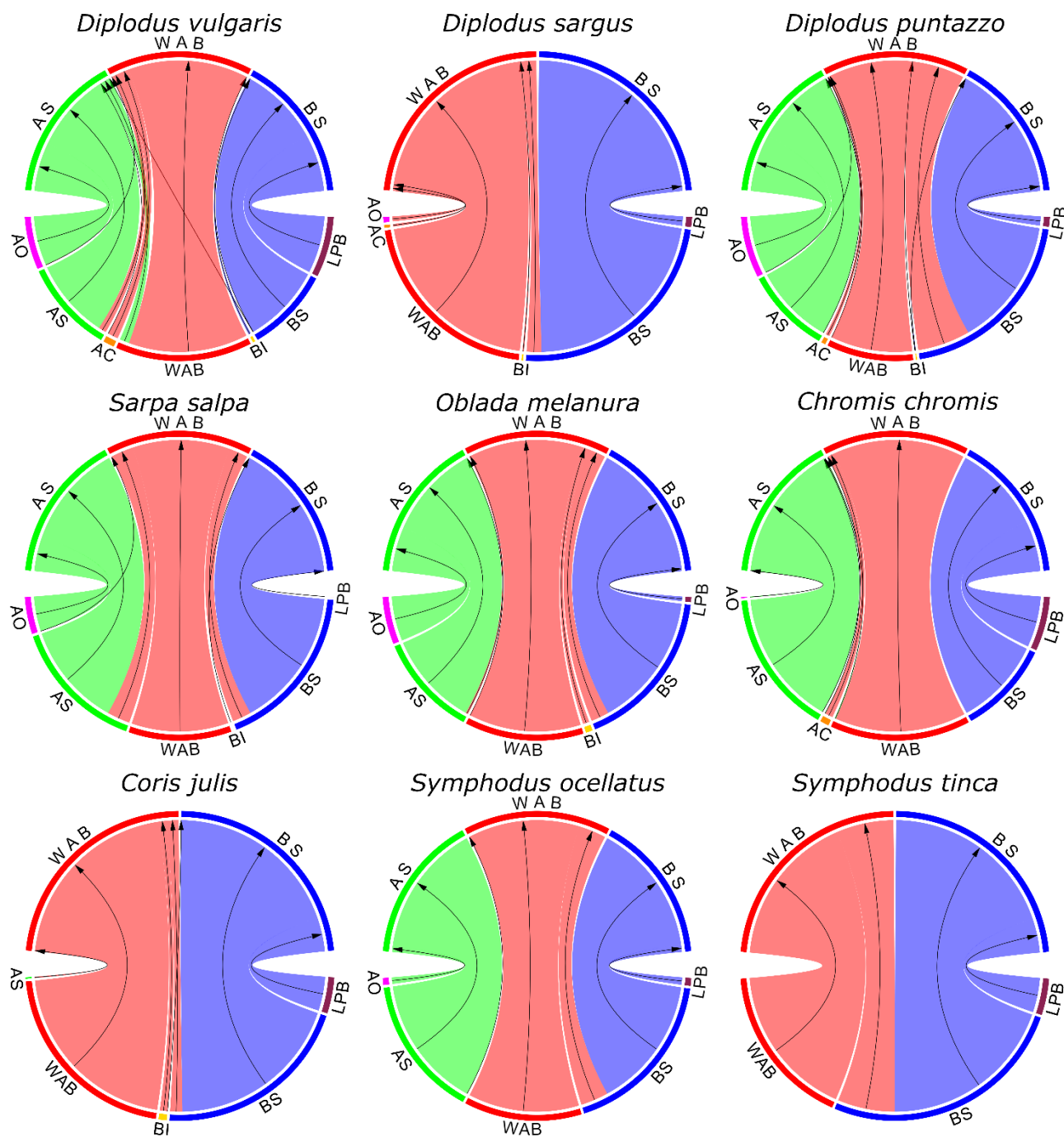
282 We generated a total of 1,413,000 backtracking trajectories from which we kept a total of 410,627  
283 trajectories originating in coastal waters (Figure 3), to be used in further analyses. Individual mean  
284 dispersal distance and orientation were calculated with these remaining trajectories, with standard  
285 deviations inside individuals around 48.3 km (min 0.3 km, max 370.6 km) for dispersal and 3.5 rad  
286 (min 0.4 rad, max 5.9 rad) for orientation. We observed that most settlers had their natal origin in the  
287 same oceanographic region where they were born (57.2%-99.9%), indicating a high level of self-  
288 recruitment at the regional level, with some differences across species and regions (Figure 4, Table  
289 S2). In the Balearic Sea, the simulations indicate that most of the settlers were from the same region

290 (85.3% ± 15.3), but some could also have arrived from the Liguro-Provençal area (14.5% ± 15.0), and  
291 a small fraction from the Balearic Islands (0.3% ± 0.6), without any contribution from other source  
292 areas. The WMOP maps showed that the Northern Current (Figure 1) exhibited a constant pattern  
293 (Figures S1). This current followed the continental slope of the North-western Mediterranean Sea from  
294 the Ligurian Sea towards the Balearic Sea and recirculated when it reached the Ibiza Channel. As  
295 expected, the proportion of settlers from the Liguro-Provençal area varied across localities and  
296 decreased from the northernmost locality (e.g. Colera) to the southernmost one (e.g. Ametlla) (Figure  
297 3). Differences among species were found from settlers originating in the Liguro-Provençal basin with  
298 a higher frequency in *D. vulgaris* and *C. chromis* (Figure 4, Table S2). Differences among species were  
299 also found for settlers originating in the Balearic Islands as for *D. puntazzo* and *D. vulgaris*, which  
300 were able to cross the Balearic Front from the Balearic Islands to the continental coast in higher  
301 frequency (Figure 3, Table S2).



302

303 Figure 3. Potential coastal origin (dots) of the settlers captured in the different sampled localities  
 304 (diamonds) as assessed by backtracking simulations for each species.



305

306 Figure 4. Dispersal plots for all nine species to the sampled areas of settlers (upper half of each circle)  
 307 from their potential source coastal areas (lower half of each circle) according to the backtracking  
 308 simulations. Arrows indicate larvae directionality and bottom bar colours delimit the source areas. AO:  
 309 Atlantic Ocean (pink), AS: Alboran Sea (green), AC: Algerian Coast (orange), WAB: West Algerian  
 310 Basin (red), BI: Balearic Islands (yellow), BS: Balearic Sea (blue), LPB: Liguro-Provençal Basin  
 311 (purple). Circle and upper bar colours indicate sampled settlement areas.



312 The Western Algerian Basin also had a high proportion of self-recruitment ( $80.1\% \pm 11.3$ ) but coupled  
313 with some incomes from other source areas (Figures 3-4). The transport across the Ibiza channel  
314 connected the Balearic Sea and the Western Algerian basin. We found a considerable potential  
315 contribution of settlers from the Balearic Sea, crossing the Ibiza Channel ( $13.9\% \pm 12.6$ ). The higher  
316 pass of larvae from the northern to the southern side of the Ibiza channel was detected in *S. tinca* and  
317 *D. puntazzo* (Figure 4, Table S2). A small contribution from the Balearic Islands was observed ( $1.0\%$   
318  $\pm 1.8$ ), being higher in *O. melanura* and *C. julis* (Figure 4). Moreover, for the three *Diplodus* species  
319 and *Chromis chromis* we detected a certain amount of settlers ( $3.4\% \pm 3$ ) from the Algerian coast  
320 (Figure 4), specially arriving at Cabo de Palos and Agua amarga sites (Figure 3). Finally, the potential  
321 proportion of settlers from the Alboran Sea through the Almeria-Oran Front was small ( $3.1\% \pm 5.3$ ).

322 The Alboran Sea was characterized by the presence of two anticyclonic gyres between Gibraltar Strait  
323 and Almeria-Oran Front. The western gyre was strong and present during the larval period of all species  
324 while the eastern gyre was milder (Figure S1). Therefore, the gyres and the AOF delimited a sub-basin  
325 that appeared to be badly connected with the rest of the Western Mediterranean Sea. However,  
326 Almeria-Oran Front decreased its strength when the eastern anticyclonic gyre faded in autumn-winter  
327 (2014-2015) allowing a transport of settlers in both directions, as it was observed during the larval  
328 period of *Diplodus vulgaris* (Figures 4, S1). A high number of settlers in the Alboran Sea were self-  
329 recruits ( $75.3\% \pm 17.8$ ), nonetheless, we found a good number of potential incoming settlers from the  
330 Atlantic Ocean through the Strait of Gibraltar ( $23.3\% \pm 16.9$ ), common in most of the species (Figure  
331 3). Thus, we can consider that the three sampling regions are three hydrodynamic units.

### 332 **3.2. Influence of early life traits on dispersal distances and orientation**

333 The global GLMM for dispersal distances explained a high proportion of the variance found in our  
334 data ( $R^2=0.814$ ). In this model, all variables (PLD, hatching date, and the two random factors, locality

335 and species) had a significant effect (Table 1). Most of the variability was explained by the random  
 336 factors, as the variance explained by the fixed factors was only  $R^2=0.045$ . The species-specific GLMM  
 337 showed that PLD positively and significantly affected dispersal distance in all species (Table 2). The  
 338 hatching date had a significant effect on dispersal distances in most species with a few exceptions as  
 339 for *Diplodus vulgaris*, *Sarpa salpa* and *Coris julis* (Table 2). The sign of the correlation changed in  
 340 some cases, for instance species such as *Diplodus sargus* and *Symphodus tinca* presented significant  
 341 negative correlations while the rest were positively correlated. Interestingly, these two species  
 342 reproduce in spring suggesting that individuals hatching early in the season disperse over larger  
 343 distances. The species with significant positive correlation (*Diplodus puntazzo*, *Oblada melanura*,  
 344 *Chromis chromis* and *Symphodus ocellatus*) reproduce, at least partially, in summer, suggesting that  
 345 individuals hatching later disperse larger distances. For all species differences between localities were  
 346 significant and the full models presented high  $R^2$  values. We observed different contribution of the  
 347 random factors across species as compared with the variance explained by their fixed factors (Table  
 348 2). For instance, in *Symphodus tinca* the variance explained by PLD and hatching date was very high  
 349 ( $R^2=0.72$ ) while in *S. ocellatus* was very low ( $R^2=0.08$ ).

350 Table 1. Results of the generalized lineal mixed model (GLMM) for the dispersal distance and dispersal  
 351 orientation We show the significance of the influence (p-value) of the fixed (PLD and Hatching date)  
 352 and random (Species and Locality) factors on dispersal distance and orientation as well as the adjusted  
 353  $R^2$  of the models including all factors (Full model) or only fixed factors.

Factors		Dispersal distance	Dispersal orientation
Fixed	PLD	< <b>2.2E-16</b>	0.395
	Hatching date	<b>1.20E-05</b>	<b>2.05E-04</b>
Random	(Species)	< <b>2.2E-16</b>	< <b>2.2e-16</b>
	(Locality)	< <b>2.2E-16</b>	< <b>2.2e-16</b>
$R^2$	Fixed factors	0.045	0.007
	Full model	0.814	0.52

354

355

356 Table 2 Results of the generalized linear mixed model (GLMM) for the dispersal distance and dispersal  
 357 orientation for each one of the studied species. We show the  $\beta$  coefficient of the influence of the fixed  
 358 factors (PLD and Hatching date), in bold when there is a significant effect. We also indicate the  
 359 influence (p-value) of Locality on dispersal distances and the adjusted  $R^2$  of the full model and only  
 360 for fixed factors.

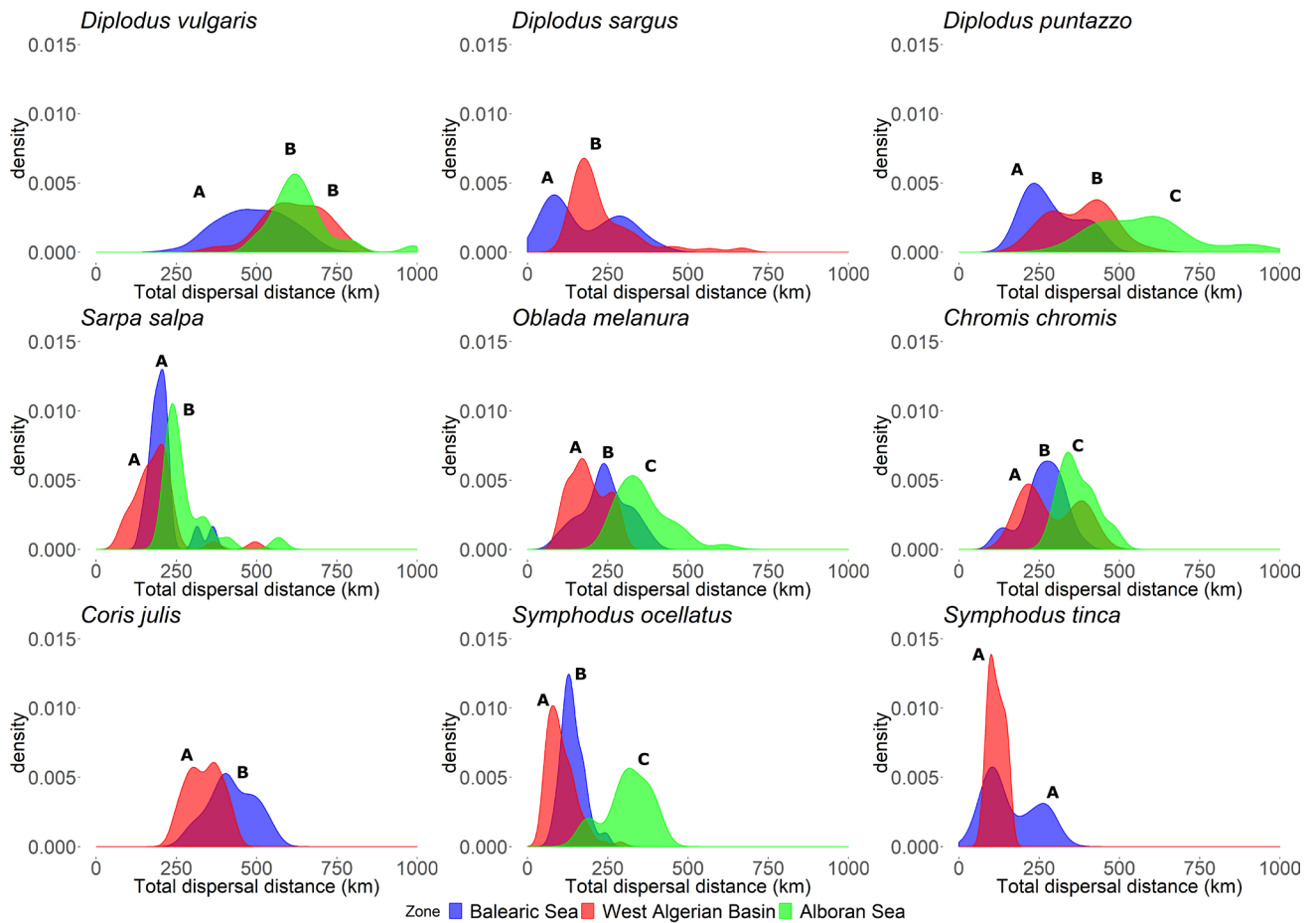
Species	Dispersal distance ~ PLD + Hatching date + (Locality)					Dispersal orientation ~ PLD + Hatching date + (Locality)				
	PLD	Hatching date	Locality	R <sup>2</sup> fixed	R <sup>2</sup> full	PLD	Hatching date	Locality	R <sup>2</sup> fixed	R <sup>2</sup> full
<i>Diplodus vulgaris</i>	<b>19.56</b>	0.31	<b>1.46E-06</b>	0.24	0.47	0.02	<b>0.55</b>	<b>7.58E-16</b>	0.03	0.58
<i>Diplodus sargus</i>	<b>20.85</b>	<b>-1.15</b>	<b>&lt; 2.2e-16</b>	0.33	0.87	- 0.02	0.44	<b>1.68E-10</b>	0.05	0.53
<i>Diplodus puntazzo</i>	<b>8.80</b>	<b>1.66</b>	<b>&lt; 2.2e-16</b>	0.03	0.67	- 0.09	0.50	<b>&lt; 2.2e-16</b>	0.01	0.67
<i>Sarpa salpa</i>	<b>18.11</b>	2.21	<b>1.21E-04</b>	0.14	0.40	- 0.14	-0.22	<b>1.01E-06</b>	0.00	0.54
<i>Oblada melanura</i>	<b>12.75</b>	<b>2.45</b>	<b>&lt; 2.2e-16</b>	0.10	0.71	- <b>0.32</b>	<b>-1.64</b>	<b>&lt; 2.2e-16</b>	0.14	0.69
<i>Chromis chromis</i>	<b>18.42</b>	<b>2.60</b>	<b>&lt; 2.2e-16</b>	0.11	0.67	- 0.20	-0.48	<b>7.24E-16</b>	0.01	0.57
<i>Coris julis</i>	<b>6.25</b>	-1.53	<b>1.70E-06</b>	0.13	0.62	0.11	-0.54	<b>1.53E-12</b>	0.03	0.53
<i>Symphodus ocellatus</i>	<b>18.47</b>	<b>0.54</b>	<b>&lt; 2.2e-16</b>	0.08	0.85	0.01	0.43	<b>6.20E-12</b>	0.02	0.44
<i>Symphodus tinca</i>	<b>19.53</b>	<b>-1.88</b>	<b>4.33E-02</b>	0.72	0.79	0.35	0.57	<b>2.55E-06</b>	0.01	0.52

361

362

363 Dispersal distances among hydrodynamic units were significantly different for most species, as  
 364 assessed with the Kruskal-Wallis and post-hoc Dunn tests (Figure 5, Table S3). Individuals settling in  
 365 the Alboran Sea showed the largest dispersal distances. The patterns in the other two basins varied  
 366 across species. Settlers of the three *Diplodus* species had significantly longer dispersal distances in the  
 367 West Algerian Basin than in the Balearic Sea, whereas *Oblada melanura*, *Chromis chromis*, *Coris julis*  
 368 and *Symphodus ocellatus* had the reverse pattern (Figure 5). *Sarpa salpa* and *Symphodus tinca* showed  
 369 no differences in mean travelled distance by recruits from these two basins.

370



371

372 Figure 5. Dispersal distance distributions of the individuals sampled in the three hydrodynamic units  
 373 based on the individual backtracking simulations for each species. Different letters within each species  
 374 indicate statistically significant differences in larval dispersal distances between hydrodynamic units  
 375 (post-hoc Dunn tests).

376

377 Dispersal orientation was significantly affected by hatching date and the two random factors (locality  
 378 and species), but not by PLD (Table 1). The full model explained a good proportion of the variance  
 379 ( $R^2=0.52$ ) although mainly due to the random factors, since the effect of the fixed factors was small  
 380 ( $R^2=0.007$ ). For the species-specific GLMM significant differences in dispersal orientation were found  
 381 among localities for each species (Table 2). However, significant effects for PLD were only found in  
 382 *O. melanura*, the correlation being negative with dispersal orientation. Thus, individuals in this species  
 383 with longer PLD originate preferentially northwards, since the 0 angle is directed to north-west and  
 384 consequently small values suggest a northern origin. The angles between 315-360 degrees which

385 indicate a northern origin could be misleading. However, only 5.34% of individuals have values in this  
386 range and therefore should not have a relevant impact on our results. The hatching date in these  
387 analyses were only significant for *O. melanura* and *D. vulgaris*, with negative and positive correlations  
388 respectively (Table 2). Consequently, in all species but *O. melanura*, the variance explained by the  
389 fixed factors on dispersal orientation was small although the full model explained a good proportion  
390 of the variance with regressions ranging from  $R^2=0.44$  in *S. ocellatus* to  $R^2=0.69$  in *O. melanura*.

391 Overall, the variance explained by PLD and hatching date on dispersal distance and orientation was  
392 small within species. However, at the individual level these two factors can have different effects in  
393 the final dispersal. For instance, individuals of *O. melanura* from Xabia with the same hatching date  
394 but different PLD had different displacement direction and longer dispersal distances with longer PLD  
395 as expected (Figure S2). Individuals from the same locality with the same PLD but different hatching  
396 date, changed also dispersal direction and distance (Figure S2). This pattern suggests that at a fine scale  
397 (*e.g.* locality scale) hatching date and PLD can have an important role in determining the origin of  
398 settlers mediated by changes in environmental conditions that at a larger scale remains undetectable.

399 The oceanographic transports during 2014-2017 showed monthly, seasonal and interannual variability  
400 across both the IC and AOF, with more stable net transports across the AOF and a higher variability  
401 across the IC (Figure S3). For each species, during its whole pelagic period, the K-W tests did not show  
402 significant differences across years in the AOF, while significant differences were observed in the IC  
403 (Table S4).

404

#### 405 **4 Discussion**

406 Here, we measured the dispersal abilities (and thus, potential connectivity) in nine common fish  
407 species in the Mediterranean Sea by individual-based simulations. We show that the three sampled

408 areas defined by the oceanographic discontinuities, Balearic Sea, West Algerian Basin and Alboran  
409 Sea, present low exchange of recruits in all species and should be considered three hydrodynamic units.  
410 Nonetheless, for some species we observed a higher directional exchange among them due to the  
411 temporal decrease in the front strength. We found significant influence of early life traits (PLD and  
412 hatching date) and sampling area in dispersal distance and orientation between and within species. Our  
413 results demonstrate that individual based information on life-history traits is fundamental to model  
414 dispersal and evaluate connectivity at a fine and regional scale.

415         The low level of larval exchange among hydrodynamic units in all species suggests that self-  
416 recruitment is the common mechanism of larval replenishment in Mediterranean coastal fishes. Using  
417 molecular techniques, such as microsatellite loci, high levels of self-recruitment had been found in  
418 some fish species in the western Mediterranean (e.g. *Tripterygion delaisi*, *Serranus cabrilla*)  
419 suggesting that a high proportion of the larvae remained close to, or never left, their natal spawning  
420 area (Carreras-Carbonell et al., 2007; Schunter et al., 2011a). Similar results were observed in coral-  
421 reef fishes (e.g. Buston and Elith, 2011; Jones et al., 2005, 1999; Swearer et al., 1999). For instance,  
422 Almany et al., 2007 found by stable isotope analyses that for species with both short (<2 weeks  
423 *Amphiprion percula*) and long (>1 month, *Chaetodon vagabundus*) PLD ca. 60% of settled juveniles  
424 were spawned at Kimbe island (Papua New Guinea), further confirmed by parentage analyses  
425 (Berumen et al., 2012; Planes et al., 2009). Similar high level of self-recruitment was observed by  
426 parentage analyses within a network of marine reserves on the Great Barrier Reef in *Plectropomus*  
427 *maculatus* and *Lutjanus carponotatus* (Harrison et al., 2012). Nevertheless, with the same assignment  
428 technique, other species showed a smaller proportion of self-recruitment in the same area, e.g.  
429 *Amphiprion polymnus* (Saenz-Agudelo et al., 2012) indicating a certain variability in these patterns  
430 probably species specific.

431 In our work, we found that the two oceanographic discontinuities present in the study area (Ibiza  
432 channel and Almeria-Oran front) determined the presence of three hydrodynamic units (Balearic Sea,  
433 West Algerian Basin and Alboran Sea) with low larval exchange in all species. Other studies have  
434 found different and larger hydrodynamic units in the same area, when simulating particle movement  
435 in different years and considering species-unspecific PLD models (Rossi et al., 2014). Temporal  
436 changes in currents and front strength in different species can account for changes in larval exchange.  
437 This seems the case of *D. vulgaris* reproducing in winter where the AOF allowed more larval exchange  
438 in both directions according to our backtracking modelling. This front had been previously reported to  
439 decrease its strength or even disappear in winter (Fernández et al., 2005; Renault et al., 2012; Tintore  
440 et al., 1988). In our study, we observed that the decrease in strength in winter of 2014-2015 was due to  
441 the fading of the eastern anticyclonic gyre in the Alboran Sea, allowing the transport of particles in  
442 both directions (Figures S1, Table S2). Nonetheless, a previous genetic study with *D. vulgaris* found  
443 strong genetic differentiation across this front (Galarza et al., 2009) suggesting that interannual  
444 variation might be relevant. Oceanographic variability across years and seasons (Botsford et al., 2009)  
445 can modify the level of self-recruitment. Inter-annual changes in gene flow across the AOF have been  
446 reported for other species such as the crab *Liocarcinus depurator* (Pascual et al., 2016), or the sea  
447 urchins *Paracentrotus lividus* (Calderón et al., 2012) and *Arbacia lixula* (Pérez-Portela et al., 2019),  
448 where temporal genetic population differentiation was associated to changes in water circulation  
449 patterns across years. Nonetheless, we did not observe significant changes in potential larval  
450 transportation across this oceanographic discontinuity during the analysed period (2014-2017)  
451 suggesting that this front is more permanent despite the reported interannual variation.

452 Oceanographic variability was also detected across the Ibiza Channel, where the meridional  
453 water transport was observed to change at weekly, seasonal and interannual scales (Balbín et al., 2014;  
454 Heslop et al., 2012; Pinot et al., 2002). We observed a high proportion of settlers in the West Algerian  
455 Basin coming from the Balearic Sea in *Symphodus tinca*, whereas in *S. ocellatus*, from the same genus

456 and with similar PLD, the proportion was lower (Figure 4). Given that these two species reproduce at  
457 different seasons, temporal seasonality in front strength can account for the capacity to cross the Ibiza  
458 Channel. This higher capacity of *S. tinca* in crossing southwards the IC is in accordance with the lower  
459 genomic differentiation found in this species in comparison to that found in *S. ocellatus* (Torrado et  
460 al., 2020). Different patterns of genetic differentiation have been reported across IC for different fish  
461 species, for instance no genetic differentiation was found for *Epinephelus marginatus* (Schunter et al.,  
462 2011b), whereas strong genetic differentiation was detected for *Serranus cabrilla* (Schunter et al.,  
463 2011a). Moreover, temporal variation has been detected in the northern site of the IC for *Liocarcinus*  
464 *depurator* further indicating that annual changes might promote differential exchange and connectivity  
465 (Pascual et al., 2016). This area is a highly dynamic transition area with variable transport in strength  
466 and direction as we have observed at different temporal scales (Figure S3) affecting dispersal patterns  
467 in all species. Therefore, the three hydrodynamic units defined in the western Mediterranean Sea by  
468 these two oceanographic discontinuities should not be considered as closed systems, but as a net with  
469 seasonally and yearly variability in connections.

470         Nevertheless, large-scale circulation patterns are not the unique factors influencing larval  
471 dispersal. In our study, we found a global relationship between early-life traits and dispersal distances  
472 and orientations. Our results demonstrate that species with longer PLD have greater dispersal distances,  
473 in accordance with previous studies (e.g. Pascual et al., 2017; Siegel et al., 2003). Moreover, hatching  
474 date also influenced dispersal distances as indicated in our global analysis, which could be related to  
475 temperature in modifying PLD through changes in larval growth rate, as with increasing temperature  
476 larvae grow quicker to their settlement size (Raventos et al., 2021; Schunter et al., 2019). Nonetheless,  
477 different impact of hatching date was obtained at the intraspecific level, with no influence for the two  
478 species with larger PLD (*D. vulgaris* and *C. julis*) and for *S. salpa*. Moreover, the regression coefficient  
479 changed in sign across species with those reproducing in spring showing negative correlations with  
480 distance so that individuals hatching earlier experience colder temperatures, show longer PLD than



481 individuals hatching later in the season and consequently disperse larger distances. Similarly *D.*  
482 *puntazzo* reproducing in autumn presents a positive correlation that could be also explain with its  
483 relation to temperature. On the other hand, those species reproducing in summer (*O. melanura*, *C.*  
484 *chromis* and *S. ocellatus*) have positive correlations, indicating that individuals hatching later have  
485 larger dispersal distances. Since temperature increases over time along this period with a corresponding  
486 decrease of PLD (Raventos et al., 2021), the effect of hatching date on dispersal distance is probably  
487 due to interaction of other factors as could be, for example, changes in productivity affecting feeding  
488 resources (Robitzch et al., 2016), but further research is necessary to unveil the causes.

489         The dispersal distances also varied at intraspecific level among our hydrodynamic units. These  
490 differences seemed to be related with two main factors: (1) differences in circulation patterns and  
491 oceanographic currents strength to which the larvae were exposed in each area, and (2) the distance  
492 and direction of available source areas of larval hatching. For instance, the larvae in the Alboran Sea  
493 had for most species longer dispersal distances than larvae in the other two areas. These longer  
494 distances were mostly due to the presence of one permanent and one semipermanent eddy in this zone  
495 (Tintore et al., 1988; present study) making larvae to travel longer distances before reaching the coast.  
496 Thus, longer dispersal distances do not imply more connectivity across hydrodynamic units since  
497 eddies can strongly contribute to self-recruitment by promoting larval retention within these areas.  
498 Moreover, eddies can further impact on populations, since they can generate recruitment peaks in  
499 punctual moments (Sponaugle et al., 2005) and increase larval development rate and settlers'  
500 survivorship (Shulzitski et al., 2016, 2015). Furthermore, the communication between Balearic Sea  
501 and Balearic Islands was probably mediated by temporal eddies occasionally formed in this area (e.g.  
502 Amores et al., 2013; Pascual et al., 2002) which can coincide with some species' larval periods as  
503 observed in our models.

504         We found that hatching date can also significantly affect dispersal orientation in the global  
505 model, and subsequently the geographic origin of settlers. However, at the intraspecific level this

506 significance was only observed in two species, *D. vulgaris* and *O. melanura* with positive and negative  
507 correlations, respectively. It is improbable that the significance in these correlations are due to sampling  
508 biases, as in six of the nine studied species we have similar number of sampling sites (6-7 localities).  
509 Furthermore, we are working at the individual level, dealing with a mean number of 150 individuals  
510 per species. Thus, individuals hatching early in the season show preferentially a southern origin in *O.*  
511 *melanura* while a northern origin in *D. vulgaris*, although this factor explained a small proportion of  
512 the model. For instance, we observed that individuals from the same locality (Xabia near the Ibiza  
513 channel) and the same PLD, but born at different dates, had a different hatching area, originating  
514 northwards or southwards. This variability could be related to daily current variations, common in  
515 coastal waters (Fernández et al., 2005), modifying dispersal orientation as observed in other species  
516 through direct dispersal assessment by parent-offspring analysis (Schunter et al., 2014). Thus, the  
517 hatching date of the individual can be more important than previously thought at a fine scale.

518

## 519 **5 Conclusions**

520 The use of oceanographic models together with PLD general information have been used in  
521 previous studies at a regional (Andrello et al., 2013; Barbut et al., 2019; Rossi et al., 2014), and global  
522 scale (Andrello et al., 2017). These studies have generated conservational strategies recommending the  
523 use of these units or cells (Boero et al., 2016) and recommended their use to establish Marine Protected  
524 Areas (MPAs) network strategies and fisheries policies (Kerr et al., 2010). In our study, both individual  
525 hatching date and PLD have been confirmed as factors to have in mind to design more precise larval  
526 dispersal models. We can conclude that having good individually otolith-inferred information about  
527 these parameters helps to a better definition of recruit's origin area and in defining hydrodynamic units.  
528 This more accurate information could be highly valuable for the identification of natural management

529 units and can be useful when considering conservation strategies such as those establishing networks  
530 of Marine Protected Areas or in defining conservation measures at regional scales.

531

## 532 **6 Acknowledgments**

533 This work was supported by the Spanish Government project ‘PopCOmics’ (CTM2017-88080)  
534 (MCIU, AEI/FEDER, UE) and by the European FP7 CoCoNet project (Ocean 2011-4, grant agreement  
535 #287844). The authors CC and MP are members of the research group SGR2017-1120 and EM of  
536 SGR2017-378 (Catalan Government). HT was supported by a PhD scholarship funded by the Spanish  
537 Ministry of Science, Innovation and Universities. The authors acknowledge the MEDCLIC project,  
538 funded by “La Caixa” Foundation, contributing to the development of the WMOP hydrodynamic  
539 model. We thank Maria Pilar Olivar and Ana Sabatés for their useful comments.

540

541

## 542 **7 References**

543

544 Aguiar, E., Mourre, B., Juza, M., Reyes, E., Hernández-Lasheras, J., Cutolo, E., Mason, E., Tintoré,  
545 J., 2020. Multi-platform model assessment in the Western Mediterranean Sea: impact of  
546 downscaling on the surface circulation and mesoscale activity. *Ocean Dyn.* 70, 273–288.  
547 <https://doi.org/10.1007/s10236-019-01317-8>

548 Allain, G., Petitgas, P., Lazure, P., Grellier, P., 2007. Biophysical modelling of larval drift, growth  
549 and survival for the prediction of anchovy (*Engraulis encrasicolus*) recruitment in the Bay of  
550 Biscay (NE Atlantic). *Fish. Oceanogr.* 16, 489–505. [https://doi.org/10.1111/j.1365-](https://doi.org/10.1111/j.1365-2419.2007.00443.x)  
551 [2419.2007.00443.x](https://doi.org/10.1111/j.1365-2419.2007.00443.x)

552 Almany, G.R., Berumen, M.L., Thorrold, S.R., Planes, S., Jones, G.P., 2007. Local replenishment of  
553 coral reef fish populations in a marine reserve. *Science* (80-. ). 316, 742–744.  
554 <https://doi.org/10.1126/science.1140597>

555 Amores, A., Monserrat, S., Marcos, M., 2013. Vertical structure and temporal evolution of an  
556 anticyclonic eddy in the Balearic Sea (western Mediterranean). *J. Geophys. Res. Ocean.* 118,  
557 2097–2106. <https://doi.org/10.1002/jgrc.20150>

- 558 Andrello, M., Guilhaumon, F., Albouy, C., Parravicini, V., Scholtens, J., Verley, P., Barange, M.,  
559 Sumaila, U.R., Manel, S., Mouillot, D., 2017. Global mismatch between fishing dependency and  
560 larval supply from marine reserves. *Nat. Commun.* 8, 1–9.  
561 <https://doi.org/10.1038/ncomms16039>
- 562 Andrello, M., Mouillot, D., Beuvier, J., Albouy, C., Thuiller, W., Manel, S., 2013. Low Connectivity  
563 between Mediterranean Marine Protected Areas: A Biophysical Modeling Approach for the  
564 Dusky Grouper *Epinephelus marginatus*. *PLoS One* 8.  
565 <https://doi.org/10.1371/journal.pone.0068564>
- 566 Andrello, M., Mouillot, D., Somot, S., Thuiller, W., Manel, S., 2015. Additive effects of climate  
567 change on connectivity between marine protected areas and larval supply to fished areas. *Divers.*  
568 *Distrib.* 21, 139–150. <https://doi.org/10.1111/ddi.12250>
- 569 Arya, S., Mount, D., Kemp, S.E., Jefferis, G., 2019. RANN: Fast Nearest Neighbour Search (Wraps  
570 ANN Library) Using L2 Metric.
- 571 Astraldi, M., Balopoulos, S., Candela, J., Font, J., Gacic, M., Gasparini, G.P., Manca, B., Theocharis,  
572 A., Tintoré, J., 1999. The role of straits and channels in understanding the characteristics of  
573 Mediterranean circulation, in: *Progress in Oceanography*. Pergamon, pp. 65–108.  
574 [https://doi.org/10.1016/S0079-6611\(99\)00021-X](https://doi.org/10.1016/S0079-6611(99)00021-X)
- 575 Ayata, S.D., Lazure, P., Thiébaud, É., 2010. How does the connectivity between populations mediate  
576 range limits of marine invertebrates? A case study of larval dispersal between the Bay of Biscay  
577 and the English Channel (North-East Atlantic). *Prog. Oceanogr.* 87, 18–36.  
578 <https://doi.org/10.1016/j.pocean.2010.09.022>
- 579 Bache, S.M., Wickham, H., 2014. magrittr: A Forward-Pipe Operator for R. R package version 1.5.  
580 Vienna, Austria R Found. Retrieved from <https://CRAN.R-project.org/package=magrittr>.
- 581 Balbín, R., López-Jurado, J.L., Flexas, M.M., Reglero, P., Vélez-Velchí, P., González-Pola, C.,  
582 Rodríguez, J.M., García, A., Alemany, F., 2014. Interannual variability of the early summer  
583 circulation around the Balearic Islands: Driving factors and potential effects on the marine  
584 ecosystem. *J. Mar. Syst.* 138, 70–81. <https://doi.org/10.1016/j.jmarsys.2013.07.004>
- 585 Banks, S.C., Piggott, M.P., Williamson, J.E., Bové, U., Holbrook, N.J., Beheregaray, L.B., 2007.  
586 Oceanic variability and coastal topography shape genetic structure in a long-dispersing sea  
587 urchin. *Ecology* 88, 3055–3064. <https://doi.org/10.1890/07-0091.1>
- 588 Barbut, L., Groot Crego, C., Delerue-Ricard, S., Vandamme, S., Volckaert, F.A.M., Lacroix, G.,  
589 2019. How larval traits of six flatfish species impact connectivity. *Limnol. Oceanogr.* 64, 1150–  
590 1171. <https://doi.org/10.1002/lno.11104>
- 591 Bates, D., Mächler, M., Bolker, B., Walker, S., 2015. Fitting Linear Mixed-Effects Models Using  
592 lme4. *J. Stat. Softw.* 67, 1–48. <https://doi.org/10.18637/jss.v067.i01>
- 593 Bauchot, M.L., 1987. Poissons osseux, Fiches FAO d'identification pour les besoins de la pêche.(rev.  
594 1). Méditerranée et mer Noire. Zone de pêche.
- 595 Berumen, M.L., Almany, G.R., Planes, S., Jones, G.P., Saenz-Agudelo, P., Thorrold, S.R., 2012.

- 596 Persistence of self-recruitment and patterns of larval connectivity in a marine protected area  
597 network. *Ecol. Evol.* 2, 444–452. <https://doi.org/10.1002/ece3.208>
- 598 Bivand, R., Keitt, T., Rowlingson, B., 2018. rgdal: Bindings for the “geospatial” data abstraction  
599 library (version 1.3-1) <https://CRAN.R-project.org/package=rgdal>.
- 600 Boero, F., Fogliani, F., Frascchetti, S., Goriup, P., Macpherson, E., Planes, S., Soukissian, T.,  
601 Consortium, C., 2016. CoCoNet: towards coast to coast networks of marine protected areas  
602 (from the shore to the high and deep sea), coupled with sea-based wind energy potential.  
603 SCIRES-IT-SCientific Res. Inf. Technol. 6, 1–95. <https://doi.org/10.2423/i22394303v6SpI>
- 604 Botsford, L.W., White, J.W., Coffroth, M.A., Paris, C.B., Planes, S., Shearer, T.L., Thorrold, S.R.,  
605 Jones, G.P., 2009. Connectivity and resilience of coral reef metapopulations in marine protected  
606 areas: Matching empirical efforts to predictive needs. *Coral Reefs*.  
607 <https://doi.org/10.1007/s00338-009-0466-z>
- 608 Bottesch, M., Gerlach, G., Halbach, M., Bally, A., Kingsford, M.J., Mouritsen, H., 2016. A magnetic  
609 compass that might help coral reef fish larvae return to their natal reef. *Curr. Biol.*  
610 <https://doi.org/10.1016/j.cub.2016.10.051>
- 611 Buston, P.M., Elith, J., 2011. Determinants of reproductive success in dominant pairs of clownfish: A  
612 boosted regression tree analysis. *J. Anim. Ecol.* 80, 528–538. <https://doi.org/10.1111/j.1365-2656.2011.01803.x>
- 614 Calderón, I., Pita, L., Brusciotti, S., Palacín, C., Turon, X., 2012. Time and space: Genetic structure  
615 of the cohorts of the common sea urchin *Paracentrotus lividus* in Western Mediterranean. *Mar.*  
616 *Biol.* 159, 187–197. <https://doi.org/10.1007/s00227-011-1799-z>
- 617 Calò, A., Lett, C., Mourre, B., Pérez-Ruzafa, Á., García-Charton, J.A., 2018. Use of Lagrangian  
618 simulations to hindcast the geographical position of propagule release zones in a Mediterranean  
619 coastal fish. *Mar. Environ. Res.* 134, 16–27. <https://doi.org/10.1016/j.marenvres.2017.12.011>
- 620 Carreras-Carbonell, J., Macpherson, E., Pascual, M., 2007. High self-recruitment levels in a  
621 Mediterranean littoral fish population revealed by microsatellite markers. *Mar. Biol.* 151, 719–  
622 727. <https://doi.org/10.1007/s00227-006-0513-z>
- 623 Christensen, A., Daewel, U., Jensen, H., Mosegaard, H., St John, M., Schrum, C., 2007.  
624 Hydrodynamic backtracking of fish larvae by individual-based modelling. *Mar. Ecol. Prog. Ser.*  
625 347, 221–232. <https://doi.org/10.3354/meps06980>
- 626 Clementi, E., Pistoia, J., Fratianni, C., Delrosso, D., Grandi, A., Drudi, M., Coppini, G., Lecci, R.,  
627 Pinaridi, N., 2017. “Mediterranean Sea Analysis and Forecast (CMEMS MED-Currents 2013-  
628 2017)”. [Data set]. Copernicus Monitoring Environment Marine Service (CMEMS).  
629 [https://doi.org/doi:10.25423/MEDSEA\\_ANALYSIS\\_FORECAST\\_PHYS\\_006\\_001](https://doi.org/doi:10.25423/MEDSEA_ANALYSIS_FORECAST_PHYS_006_001)
- 630 Cowen, R.K., 2002. Oceanographic Influences on Larval Dispersal and Retention and Their  
631 Consequences for Population Connectivity.
- 632 Cowen, R.K., Sponaugle, S., 2009. Larval dispersal and marine population connectivity. *Ann. Rev.*  
633 *Mar. Sci.* 1, 443–466. <https://doi.org/10.1146/annurev.marine.010908.163757>

- 634 Di Franco, A., Gillanders, B.M., de Benedetto, G., Pennetta, A., de Leo, G.A., Guidetti, P., 2012.  
635 Dispersal patterns of coastal fish: Implications for designing networks of marine protected areas.  
636 PLoS One 7. <https://doi.org/10.1371/journal.pone.0031681>
- 637 Döös, K., Engqvist, A., 2007. Assessment of water exchange between a discharge region and the  
638 open sea – A comparison of different methodological concepts. *Estuar. Coast. Shelf Sci.* 74,  
639 709–721. <https://doi.org/10.1016/j.ecss.2007.05.022>
- 640 Döös, K., Jönsson, B., 2013. TRACMASS—A lagrangian trajectory model, in: *Preventive Methods  
641 for Coastal Protection: Towards the Use of Ocean Dynamics for Pollution Control*. Springer  
642 International Publishing, pp. 225–249. [https://doi.org/10.1007/978-3-319-00440-2\\_7](https://doi.org/10.1007/978-3-319-00440-2_7)
- 643 Döös, K., Rupolo, V., Brodeau, L., 2011. Dispersion of surface drifters and model-simulated  
644 trajectories. *Ocean Model.* 39, 301–310. <https://doi.org/10.1016/j.ocemod.2011.05.005>
- 645 Faillettaz, R., Blandin, A., Paris, C.B., Koubbi, P., Irisson, J.O., 2015. Sun-compass orientation in  
646 mediterranean fish larvae. *PLoS One* 10, e0135213.  
647 <https://doi.org/10.1371/journal.pone.0135213>
- 648 Faillettaz, R., Durand, E., Paris, C.B., Koubbi, P., Irisson, J.O., 2018. Swimming speeds of  
649 Mediterranean settlement-stage fish larvae nuance Hjort’s aberrant drift hypothesis. *Limnol.  
650 Oceanogr.* 63, 509–523. <https://doi.org/10.1002/lno.10643>
- 651 Fernández, V., Dietrich, D.E., Haney, R.L., Tintoré, J., 2005. Mesoscale, seasonal and interannual  
652 variability in the Mediterranean Sea using a numerical ocean model. *Prog. Oceanogr.* 66, 321–  
653 340. <https://doi.org/10.1016/j.pocean.2004.07.010>
- 654 Fraker, M.E., Anderson, E.J., Brodnik, R.M., Carreon-Martinez, L., DeVanna, K.M., Fryer, B.J.,  
655 Heath, D.D., Reichert, J.M., Ludsin, S.A., 2015. Particle backtracking improves breeding  
656 subpopulation discrimination and natal-source identification in mixed populations. *PLoS One*  
657 10. <https://doi.org/10.1371/journal.pone.0120752>
- 658 Gaines, S.D., Gaylord, B., Gerber, L.R., Hastings, A., Kinlan, B.P., 2007. Connecting places: The  
659 ecological consequences of dispersal in the sea. *Oceanography* 20, 90–99.  
660 <https://doi.org/10.5670/oceanog.2007.32>
- 661 Galarza, J.A., Carreras-Carbonell, J., Macpherson, E., Pascual, M., Roques, S., Turner, G.F., Rico,  
662 C., 2009. The influence of oceanographic fronts and early-life-history traits on connectivity  
663 among littoral fish species. *Proc. Natl. Acad. Sci.* 106, 1473–1478.  
664 <https://doi.org/10.1073/pnas.0806804106>
- 665 Garcia Lafuente, J., Lopez Jurado, J.L., Cano Lucaya, N., Vargas Yanez, M., Aguiar Garcia, J., 1995.  
666 Circulation of water masses through the Ibiza Channel. *Oceanol. Acta* 18, 245–254.
- 667 Garnier, S., 2018. viridis: Default Color Maps from “matplotlib.”
- 668 Gu, Z., Gu, L., Eils, R., Schlesner, M., Brors, B., 2014. Circlize implements and enhances circular  
669 visualization in R. *Bioinformatics* 30, 2811–2812. <https://doi.org/10.1093/bioinformatics/btu393>
- 670 Harrison, H.B., Williamson, D.H., Evans, R.D., Almany, G.R., Thorrold, S.R., Russ, G.R., Feldheim,

- 671 K.A., Van Herwerden, L., Planes, S., Srinivasan, M., Berumen, M.L., Jones, G.P., 2012. Larval  
672 export from marine reserves and the recruitment benefit for fish and fisheries. *Curr. Biol.* 22,  
673 1023–1028. <https://doi.org/10.1016/j.cub.2012.04.008>
- 674 Heslop, E.E., Ruiz, S., Allen, J., López-Jurado, J.L., Renault, L., Tintoré, J., 2012. Autonomous  
675 underwater gliders monitoring variability at choke points in our ocean system: A case study in  
676 the Western Mediterranean Sea. *Geophys. Res. Lett.* 39, 1–6.  
677 <https://doi.org/10.1029/2012GL053717>
- 678 Holliday, D., Beckley, L., Millar, N., Olivar, M., Slawinski, D., Feng, M., Thompson, P., 2012.  
679 Larval fish assemblages and particle back-tracking define latitudinal and cross-shelf variability  
680 in an eastern Indian Ocean boundary current. *Mar. Ecol. Prog. Ser.* 460, 127–144.  
681 <https://doi.org/10.3354/meps09730>
- 682 Jones, G.P., Millcich, M.J., Emsile, M.J., Lunow, C., 1999. Self-recruitment in a coral fish  
683 population. *Nature* 402, 802–804. <https://doi.org/10.1038/45538>
- 684 Jones, G.P., Planes, S., Thorrold, S.R., 2005. Coral reef fish larvae settle close to home. *Curr. Biol.*  
685 15, 1314–1318. <https://doi.org/10.1016/j.cub.2005.06.061>
- 686 Juza, M., Escudier, R., Vargas-Yáñez, M., Mourre, B., Heslop, E., Allen, J., Tintoré, J., 2019.  
687 Characterization of changes in Western Intermediate Water properties enabled by an innovative  
688 geometry-based detection approach. *J. Mar. Syst.* 191, 1–12.  
689 <https://doi.org/10.1016/j.jmarsys.2018.11.003>
- 690 Juza, M., Mourre, B., Renault, L., Gómara, S., Sebastian, K., López, S.L., Borrueco, B.F., Beltran,  
691 J.P., Troupin, C., Tomás, M.T., others, 2016. Operational SOCIB forecasting system and multi-  
692 platform validation in the Western Mediterranean. *J. Oper. Ocean.* 9, 9231.
- 693 Kerr, L.A., Cadrin, S.X., Secor, D.H., 2010. Simulation modelling as a tool for examining the  
694 consequences of spatial structure and connectivity on local and regional population dynamics.  
695 *ICES J. Mar. Sci.* 67, 1631–1639. <https://doi.org/10.1093/icesjms/fsq053>
- 696 Kingsford, M.J., Leis, J.M., Shanks, A., Lindeman, K.C., Morgan, S.G., Pineda, J., 2002. Sensory  
697 environments, larval abilities and local self-recruitment. *Bull. Mar. Sci.*
- 698 Kinlan, B.P., Gaines, S.D., Lester, S.E., 2005. Propagule dispersal and the scales of marine  
699 community process. *Divers. Distrib.* 11, 139–148. [https://doi.org/10.1111/j.1366-  
700 9516.2005.00158.x](https://doi.org/10.1111/j.1366-9516.2005.00158.x)
- 701 Kough, A.S., Paris, C.B., 2015. The influence of spawning periodicity on population connectivity.  
702 *Coral Reefs* 34, 753–757. <https://doi.org/10.1007/s00338-015-1311-1>
- 703 Leis, J.M., 2007. Behaviour as input for modelling dispersal of fish larvae: Behaviour, biogeography,  
704 hydrodynamics, ontogeny, physiology and phylogeny meet hydrography. *Mar. Ecol. Prog. Ser.*  
705 <https://doi.org/10.3354/meps06977>
- 706 Leis, J.M., 1991. The pelagic stage of reef fishes: the larval biology of coral fishes. *Ecol. fishes coral*  
707 *reefs.*

- 708 Leis, J.M., Hay, A.C., Gaither, M.R., 2011. Swimming ability and its rapid decrease at settlement in  
709 wrasse larvae (Teleostei: Labridae). *Mar. Biol.* 158, 1239–1246. [https://doi.org/10.1007/s00227-](https://doi.org/10.1007/s00227-011-1644-4)  
710 011-1644-4
- 711 Leis, J.M., Paris, C.B., Irisson, J.O., Yerman, M.N., Siebeck, U.E., 2014. Orientation of fish larvae in  
712 situ is consistent among locations, years and methods, but varies with time of day. *Mar. Ecol.*  
713 *Prog. Ser.* 505, 193–208. <https://doi.org/10.3354/meps10792>
- 714 Millot, C., 1999. Circulation in the Western Mediterranean Sea. *J. Mar. Syst.* 20, 423–442.  
715 [https://doi.org/10.1016/S0924-7963\(98\)00078-5](https://doi.org/10.1016/S0924-7963(98)00078-5)
- 716 Millot, C., Taupier-Letage, I., 2005. Circulation in the Mediterranean Sea, in: Saliot, A. (Ed.), *The*  
717 *Mediterranean Sea*. Springer Berlin Heidelberg, Berlin, Heidelberg, pp. 29–66.  
718 <https://doi.org/10.1007/b107143>
- 719 Mouritsen, H., Atema, J., Kingsford, M.J., Gerlach, G., 2013. Sun Compass Orientation Helps Coral  
720 Reef Fish Larvae Return to Their Natal Reef. *PLoS One* 8.  
721 <https://doi.org/10.1371/journal.pone.0066039>
- 722 Mourre, B., Aguiar, E., Juza, M., Hernandez-Lasheras, J., Reyes, E., Heslop, E., Escudier, R., Cutolo,  
723 E., Ruiz, S., Mason, E., Pascual, A., Tintoré, J., 2018. Assessment of High-Resolution Regional  
724 Ocean Prediction Systems Using Multi-Platform Observations: Illustrations in the Western  
725 Mediterranean Sea, in: *New Frontiers in Operational Oceanography*. pp. 663–694.  
726 <https://doi.org/10.17125/gov2018.ch24>
- 727 O’Connor, J., Muheim, R., 2017. Pre-settlement coral-reef fish larvae respond to magnetic field  
728 changes during the day. *J. Exp. Biol.* 220, 2874–2877. <https://doi.org/10.1242/jeb.159491>
- 729 Olivar, M.P., Emelianov, M., Villate, F., Uriarte, I., Maynou, F., Álvarez, I., Morote, E., 2010. The  
730 role of oceanographic conditions and plankton availability in larval fish assemblages off the  
731 Catalan coast (NW Mediterranean). *Fish. Oceanogr.* 19, 209–229.  
732 <https://doi.org/10.1111/j.1365-2419.2010.00538.x>
- 733 Ospina-Alvarez, A., Catalán, I.A., Bernal, M., Roos, D., Palomera, I., 2015. From egg production to  
734 recruits: Connectivity and inter-annual variability in the recruitment patterns of European  
735 anchovy in the northwestern Mediterranean. *Prog. Oceanogr.* 138, 431–447.  
736 <https://doi.org/10.1016/j.pocean.2015.01.011>
- 737 Paris, C.B., Atema, J., Irisson, J.O., Kingsford, M., Gerlach, G., Guigand, C.M., 2013. Reef Odor: A  
738 Wake Up Call for Navigation in Reef Fish Larvae. *PLoS One* 8, e72808.  
739 <https://doi.org/10.1371/journal.pone.0072808>
- 740 Paris, C.B., Cowen, R.K., 2004. Direct evidence of a biophysical retention mechanism for coral reef  
741 fish larvae. *Limnol. Oceanogr.* 49, 1964–1979. <https://doi.org/10.4319/lo.2004.49.6.1964>
- 742 Pascual, A., Buongiorno Nardelli, B., Larnicol, G., Emelianov, M., Gomis, D., 2002. A case of an  
743 intense anticyclonic eddy in the Balearic Sea (western Mediterranean). *J. Geophys. Res. C*  
744 *Ocean.* 107, 4–1. <https://doi.org/10.1029/2001jc000913>
- 745 Pascual, M., Palero, F., García-Merchán, V.H., Macpherson, E., Robainas-Barcia, A., Mestres, F.,



- 746 Roda, T., Abelló, P., 2016. Temporal and spatial genetic differentiation in the crab *Liocarcinus*  
747 *depurator* across the Atlantic-Mediterranean transition. *Sci. Rep.* 6, 1–10.  
748 <https://doi.org/10.1038/srep29892>
- 749 Pascual, M., Rives, B., Schunter, C., Macpherson, E., 2017. Impact of life history traits on gene flow:  
750 A multispecies systematic review across oceanographic barriers in the Mediterranean Sea. *PLoS*  
751 *One* 12, 1–20. <https://doi.org/10.1371/journal.pone.0176419>
- 752 Payne, M.R., Ross, S.D., Clausen, L.W., Munk, P., Mosegaard, H., Nash, R.D.M., 2013. Recruitment  
753 decline in North Sea herring is accompanied by reduced larval growth rates. *Mar. Ecol. Prog.*  
754 *Ser.* 489, 197–211. <https://doi.org/10.3354/meps10392>
- 755 Pérez-Portela, R., Wangensteen, O.S., Garcia-Cisneros, A., Valero-Jiménez, C., Palacín, C., Turon,  
756 X., 2019. Spatio-temporal patterns of genetic variation in *Arbacia lixula*, a thermophilous sea  
757 urchin in expansion in the Mediterranean. *Heredity (Edinb)*. 122, 244–259.  
758 <https://doi.org/10.1038/s41437-018-0098-6>
- 759 Pierce, D., 2017. ncd4: interface to Unidata netCDF (version 4 or earlier) format data files.--R  
760 package ver. 1.16.
- 761 Pinot, J.M., López-Jurado, J.L., Riera, M., 2002. The CANALES experiment (1996-1998).  
762 Interannual, seasonal, and mesoscale variability of the circulation in the Balearic Channels.  
763 *Prog. Oceanogr.* [https://doi.org/10.1016/S0079-6611\(02\)00139-8](https://doi.org/10.1016/S0079-6611(02)00139-8)
- 764 Planes, S., Jones, G.P., Thorrold, S.R., 2009. Larval dispersal connects fish populations in a network  
765 of marine protected areas. *Proc. Natl. Acad. Sci. U. S. A.* 106, 5693–5697.  
766 <https://doi.org/10.1073/pnas.0808007106>
- 767 R Core Team, 2018. R: A Language and Environment for Statistical Computing.
- 768 Raventos, N., Macpherson, E., 2005. Effect of pelagic larval growth and size-at-hatching on post-  
769 settlement survivorship in two temperate labrid fish of the genus *Symphodus*. *Mar. Ecol. Prog.*  
770 *Ser.* 285, 205–211. <https://doi.org/10.3354/meps285205>
- 771 Raventos, N., Macpherson, E., 2001. Planktonic larval duration and settlement marks on the otoliths  
772 of Mediterranean littoral fishes. *Mar. Biol.* 138, 1115–1120.  
773 <https://doi.org/10.1007/s002270000535>
- 774 Raventos, N., Torrado, H., Arthur, R., Alcoverro, T., Macpherson, E., 2021. Temperature reduces  
775 fish dispersal as larvae grow faster to their settlement size. *J. Anim. Ecol.*
- 776 Renault, L., Oguz, T., Pascual, A., Vizoso, G., Tintore, J., 2012. Surface circulation in the Alboran  
777 Sea (western Mediterranean) inferred from remotely sensed data. *J. Geophys. Res. Ocean.* 117.  
778 <https://doi.org/10.1029/2011JC007659>
- 779 Robitzch, V.S.N., Lozano-Cortés, D., Kandler, N.M., Salas, E., Berumen, M.L., 2016. Productivity  
780 and sea surface temperature are correlated with the pelagic larval duration of damselfishes in the  
781 Red Sea. *Mar. Pollut. Bull.* 105, 566–574. <https://doi.org/10.1016/j.marpollbul.2015.11.045>
- 782 Ross, S.D., Payne, M.R., Worsøe Clausen, L., Munk, P., Mosegaard, H., Nash, R.D.M., 2012.

- 783 Coupling otolith microstructure analysis and hydrographic backtracking suggests a mechanism  
784 for the 2000s North Sea herring recruitment failure. *ICES C.* 2012/J 14, 33.
- 785 Rossi, V., Ser-Giacomi, E., L pez, C., Hern ndez-Garc a, E., 2014. Hydrodynamic provinces and  
786 oceanic connectivity from a transport network help designing marine reserves. *Geophys. Res.*  
787 *Lett.* 41, 2883–2891. <https://doi.org/10.1002/2014GL059540>
- 788 Sabat s, A., Olivar, M.P., 1996. Variation of larval fish distributions associated with variability in the  
789 location of a shelf-slope front. *Mar. Ecol. Prog. Ser.* 135, 11–20.  
790 <https://doi.org/10.3354/meps135011>
- 791 Saenz-Agudelo, P., Jones, G.P., Thorrold, S.R., Planes, S., 2012. Patterns and persistence of larval  
792 retention and connectivity in a marine fish metapopulation. *Mol. Ecol.* 21, 4695–4705.  
793 <https://doi.org/10.1111/j.1365-294X.2012.05726.x>
- 794 Salat, J., 1996. Review of hydrographic environmental factors that may influence anchovy habitats in  
795 northwestern Mediterranean. *Sci. Mar.* 60, 21–32.
- 796 Schneider, W., 1990. Field guide to the commercial marine resources of the Gulf of Guinea. FAO  
797 species identification sheets for fishery purposes.
- 798 Schunter, C., Carreras-Carbonell, J., Macpherson, E., Tintor , J., Vidal-Vijande, E., Pascual, A.,  
799 Guidetti, P., Pascual, M., 2011a. Matching genetics with oceanography: Directional gene flow  
800 in a Mediterranean fish species. *Mol. Ecol.* 20, 5167–5181. <https://doi.org/10.1111/j.1365-294X.2011.05355.x>  
801
- 802 Schunter, C., Carreras-Carbonell, J., Planes, S., Sala, E., Ballesteros, E., Zabala, M., Harmelin, J.G.,  
803 Harmelin-Vivien, M., Macpherson, E., Pascual, M., 2011b. Genetic connectivity patterns in an  
804 endangered species: The dusky grouper (*Epinephelus marginatus*). *J. Exp. Mar. Bio. Ecol.* 401,  
805 126–133. <https://doi.org/10.1016/j.jembe.2011.01.021>
- 806 Schunter, C., Pascual, M., Garza, J.C., Raventos, N., Macpherson, E., 2014. Kinship analyses  
807 identify fish dispersal events on a temperate coastline. *Proc. R. Soc. B Biol. Sci.* 281.  
808 <https://doi.org/10.1098/rspb.2014.0556>
- 809 Schunter, C., Pascual, M., Raventos, N., Garriga, J., Garza, J.C., Bartumeus, F., Macpherson, E.,  
810 2019. A novel integrative approach elucidates fine-scale dispersal patchiness in marine  
811 populations. *Sci. Rep.* 9, 1–10. <https://doi.org/10.1038/s41598-019-47200-w>
- 812 Selkoe, K.A., Toonen, R.J., 2011. Marine connectivity: A new look at pelagic larval duration and  
813 genetic metrics of dispersal. *Mar. Ecol. Prog. Ser.* 436, 291–305.  
814 <https://doi.org/10.3354/meps09238>
- 815 Selkoe, K.A., Watson, J.R., White, C., Horin, T. Ben, Iacchei, M., Mitarai, S., Siegel, D.A., Gaines,  
816 S.D., Toonen, R.J., 2010. Taking the chaos out of genetic patchiness: Seascape genetics reveals  
817 ecological and oceanographic drivers of genetic patterns in three temperate reef species. *Mol.*  
818 *Ecol.* 19, 3708–3726. <https://doi.org/10.1111/j.1365-294X.2010.04658.x>
- 819 Shanks, A.L., 2009. Pelagic Larval Duration and Dispersal Distance Revisited. *Biol. Bull.* 216, 373–  
820 385. <https://doi.org/10.1086/bblv216n3p373>

- 821 Shanks, A.L., Brink, L., 2005. Upwelling, downwelling, and cross-shelf transport of bivalve larvae:  
822 Test of a hypothesis. *Mar. Ecol. Prog. Ser.* 302, 1–12. <https://doi.org/10.3354/meps302001>
- 823 Shulzitski, K., Sponaugle, S., Hauff, M., Walter, K., D’Alessandro, E.K., Cowen, R.K., 2015. Close  
824 encounters with eddies: Oceanographic features increase growth of larval reef fishes during their  
825 journey to the reef. *Biol. Lett.* 11. <https://doi.org/10.1098/rsbl.2014.0746>
- 826 Shulzitski, K., Sponaugle, S.S., Hauff, M., Walter, K.D., Cowen, R.K., 2016. Encounter with  
827 mesoscale eddies enhances survival to settlement in larval coral reef fishes. *Proc. Natl. Acad.*  
828 *Sci. U. S. A.* 113, 6928–6933. <https://doi.org/10.1073/pnas.1601606113>
- 829 Siegel, D.A., Kinlan, B.P., Gaylord, B., Gaines, S.D., 2003. Lagrangian descriptions of marine larval  
830 dispersion. *Mar. Ecol. Prog. Ser.* 260, 83–96. <https://doi.org/10.3354/meps260083>
- 831 Sponaugle, S., Cowen, R.K., 1996. Larval supply and patterns of recruitment for two caribbean reef  
832 fishes, *Stegastes partitus* and *Acanthurus bahianus*, in: *Marine and Freshwater Research*.  
833 CSIRO, pp. 433–447. <https://doi.org/10.1071/MF9960433>
- 834 Sponaugle, Su, Cowen, R.K., 1996. Larval supply and patterns of recruitment for two caribbean reef  
835 fishes, *Stegastes partitus* and *Acanthurus bahianus*, in: *Marine and Freshwater Research*.  
836 CSIRO, pp. 433–447. <https://doi.org/10.1071/MF9960433>
- 837 Sponaugle, S., Lee, T., Kourafalou, V., Pinkard, D., 2005. Florida Current frontal eddies and the  
838 settlement of coral reef fishes. *Limnol. Oceanogr.* 50, 1033–1048.  
839 <https://doi.org/10.4319/lo.2005.50.4.1033>
- 840 Staaterman, E., Paris, C.B., Helgers, J., 2012. Orientation behavior in fish larvae: A missing piece to  
841 Hjort’s critical period hypothesis. *J. Theor. Biol.* 304, 188–196.  
842 <https://doi.org/10.1016/j.jtbi.2012.03.016>
- 843 Swearer, S.E., Caselle, J.E., Lea, D.W., Warner, R.R., 1999. Larval retention and recruitment in an  
844 island population of a coral-reef fish. *Nature* 402, 799–802. <https://doi.org/10.1038/45533>
- 845 Thyng, K., Hetland, R., 2014. TracPy: Wrapping the Fortran Lagrangian trajectory model  
846 TRACMASS, in: *Proceedings of the 13th Python in Science Conference*. pp. 79–84.  
847 <https://doi.org/10.25080/majora-14bd3278-00d>
- 848 Tintore, J., La Violette, P.E., Blade, I., Cruzado, A., 1988. A Study of an Intense Density Front in the  
849 Eastern Alboran Sea: The Almeria–Oran Front. *J. Phys. Oceanogr.* 18, 1384–1397.  
850 [https://doi.org/10.1175/1520-0485\(1988\)018<1384:asoaid>2.0.co;2](https://doi.org/10.1175/1520-0485(1988)018<1384:asoaid>2.0.co;2)
- 851 Tintoré, J., Pinardi, N., Álvarez-Fanjul, E., Aguiar, E., Álvarez-Berastegui, D., Bajo, M., Balbin, R.,  
852 Bozzano, R., Nardelli, B.B., Cardin, V., Casas, B., Charcos-Llorens, M., Chiggiato, J.,  
853 Clementi, E., Coppini, G., Coppola, L., Cossarini, G., Deidun, A., Deudero, S., D’Ortenzio, F.,  
854 Drago, A., Drudi, M., El Serafy, G., Escudier, R., Farcy, P., Federico, I., Fernández, J.G.,  
855 Ferrarin, C., Fossi, C., Frangoulis, C., Galgani, F., Gana, S., García Lafuente, J., Sotillo, M.G.,  
856 Garreau, P., Gertman, I., Gómez-Pujol, L., Grandi, A., Hayes, D., Hernández-Lasheras, J.,  
857 Herut, B., Heslop, E., Hilmi, K., Juza, M., Kallos, G., Korres, G., Lecci, R., Lazzari, P., Lorente,  
858 P., Liubartseva, S., Louanchi, F., Malacic, V., Mannarini, G., March, D., Marullo, S., Mauri, E.,  
859 Meszaros, L., Mourre, B., Mortier, L., Muñoz-Mas, C., Novellino, A., Obaton, D., Orfila, A.,

- 860 Pascual, A., Pensieri, S., Pérez Gómez, B., Pérez Rubio, S., Perivoliotis, L., Petihakis, G., de la  
861 Villéon, L.P., Pistoia, J., Poulain, P.M., Pouliquen, S., Prieto, L., Raimbault, P., Reglero, P.,  
862 Reyes, E., Rotllan, P., Ruiz, S., Ruiz, J., Ruiz, I., Ruiz-Orejón, L.F., Salihoglu, B., Salon, S.,  
863 Sammartino, S., Sánchez Arcilla, A., Sannino, G., Sannino, G., Santoleri, R., Sardá, R.,  
864 Schroeder, K., Simoncelli, S., Sofianos, S., Sylaios, G., Tanhua, T., Teruzzi, A., Testor, P.,  
865 Tezcan, D., Torner, M., Trotta, F., Umgiesser, G., von Schuckmann, K., Verri, G., Vilibic, I.,  
866 Yucel, M., Zavatarelli, M., Zodiatis, G., 2019. Challenges for Sustained Observing and  
867 Forecasting Systems in the Mediterranean Sea. *Front. Mar. Sci.* 6.  
868 <https://doi.org/10.3389/fmars.2019.00568>
- 869 Tintoré, J., Vizoso, G., Casas, B., Heslop, E., Pascual, A., Orfila, A., Ruiz, S., Martínez-Ledesma,  
870 M., Torner, M., Cusí, S., Diedrich, A., Balaguer, P., Gómez-Pujol, L., Álvarez-Ellacuria, A.,  
871 Gómara, S., Sebastian, K., Lora, S., Beltrán, J.P., Renault, L., Juzà, M., Álvarez, D., March, D.,  
872 Garau, B., Castilla, C., Cañellas, T., Roque, D., Lizarán, I., Pitarch, S., Carrasco, M.A., Lana,  
873 A., Mason, E., Escudier, R., Conti, D., Sayol, J.M., Barceló, B., Alemany, F., Reglero, P.,  
874 Massuti, E., Vélez-Belchí, P., Ruiz, J., Oguz, T., Gómez, M., Álvarez, E., Ansorena, L.,  
875 Manriquez, M., 2013. SOCIB: The Balearic Islands Coastal Ocean Observing and Forecasting  
876 System Responding to Science, Technology and Society Needs. *Mar. Technol. Soc. J.* 47, 101–  
877 117. <https://doi.org/10.4031/MTSJ.47.1.10>
- 878 Torrado, H., Carreras, C., Raventos, N., Macpherson, E., Pascual, M., 2020. Individual-based  
879 population genomics reveal different drivers of adaptation in sympatric fish. *Sci. Rep.*  
880 <https://doi.org/10.1038/s41598-020-69160-2>
- 881 Treml, E.A., Roberts, J.J., Chao, Y., Halpin, P.N., Possingham, H.P., Riginos, C., 2012.  
882 Reproductive output and duration of the pelagic larval stage determine seascape-wide  
883 connectivity of marine populations, in: *Integrative and Comparative Biology*. Narnia, pp. 525–  
884 537. <https://doi.org/10.1093/icb/ics101>
- 885 White, J.W., Carr, M.H., Caselle, J.E., Washburn, L., Woodson, C.B., Palumbi, S.R., Carlson, P.M.,  
886 Warner, R.R., Menge, B.A., Barth, J.A., Blanchette, C.A., Raimondi, P.T., Milligan, K., 2019.  
887 Connectivity, dispersal, and recruitment: Connecting benthic communities and the coastal  
888 ocean. *Oceanography* 32, 50–59. <https://doi.org/10.5670/oceanog.2019.310>
- 889 Wickham, H., 2016. *ggplot2: Elegant Graphics for Data Analysis*. Springer-Verlag New York.
- 890 Wickham, H., 2007. Reshaping data with the reshape package. *J. Stat. Softw.* 21, 1–20.
- 891 Wickham, H., François, R., Henry, L., Müller, K., 2018. *Dplyr: A Grammar of Data Manipulation*; R  
892 Package Version 0.7. 8.
- 893 Wilson, McCormick, M.I., 1999. Microstructure of settlement-marks in the otoliths of tropical reef  
894 fishes. *Mar. Biol.* 134, 29–41. <https://doi.org/10.1007/s002270050522>
- 895